6 Sobue G, Hashizume Y, Mukai E, Hirayama M, Mitsuma T, Takahashi A. X-linked recessive bulbospinal neuronopathy. A clinicopathological study. *Brain* 1989; **112**: 209–32
7 Lee JH, Shin JH, Park KP, Kim IJ, Kim CM, Lim JG, Choi YC, Kim DS. Phenotypic variability in Kennedy's disease: implication of the early diagnostic features. *Acta Neurol Scand* 2005; **112**: 57–63
8 Atsuta N, Watanabe H, Ito M, Banno H, Suzuki K, Katsuno M, Tanaka F, Tamakoshi A, Sobue G. Natural history of spinal and bulbar muscular atrophy (SBMA). A study of 223 Japanese patients. *Brain* 2006; **129**: 1446–55
9 Arbizu T, Santamaria J, Gomez JM, Quilez A, Serra JP. A family with adult spinal and bulbar muscular atrophy, X-linked inheritance and associated testicular failure. *J Neurol Sci* 1983; **59**: 371–82
10 Hausmanowa-Petrusewicz I, Borkowska J, Janczewski Z. X-linked adult form of spinal muscular atrophy. *J Neurol* 1983; **229**: 175–88
11 Nagashima T, Seko K, Hirose K, Mannen T, Yoshimura S, Arima R, Nagashima K, Morimatsu Y. Familial bulbospinal muscular atrophy associated with testicular atrophy and sensory neuropathy (Kennedy–Alter–Sung syndrome). Autopsy case report of two brothers. *J Neurol Sci* 1988; **87**: 141–52
12 Echaniz-Laguna A, Rousso E, Anheim M, Cossee M, Tranchant C. A family with early-onset and rapidly progressive X-linked spinal and bulbar muscular atrophy. *Neurology* 2005; **64**: 1458–60
13 Danek A, Witt TN, Mann K, Schweikert HU, Romalo G, La Spada AR, Fischbeck KH. Decrease in androgen binding and effect of androgen treatment in a case of X-linked bulbospinal neuronopathy. *Clin Invest* 1994; **72**: 892–7
14 Goldenberg JN, Bradley WG. Testosterone therapy and the pathogenesis of Kennedy's disease (X-linked bulbospinal muscular atrophy). *J Neurol Sci* 1996; **135**: 158–61
15 Neuschmid-Kaspar F, Gast A, Peterziel H, Schneikert J, Muigg A, Ransmayr G, Klocker H, Bartsch G, Cato AC. CAG-repeat expansion in androgen receptor in Kennedy's disease is not a loss of function mutation. *Mol Cell Endocrinol* 1996; **117**: 149–56
16 Antonini G, Gragnani F, Romaniello A, Pennisi EM, Morino S, Ceschin V, Santoro L, Cruccu G. Sensory involvement in spinal-bulbar muscular atrophy (Kennedy's disease). *Muscle Nerve* 2000; **23**: 252–8
17 Lieberman AP, Fischbeck KH. Triplet repeat expansion in neuromuscular disease. *Muscle Nerve* 2000; **23**: 843–50
18 Sinnreich M, Sorenson EJ, Klein CJ. Neurologic course, endocrine dysfunction and triplet repeat size in spinal bulbar muscular atrophy. *Can J Neurol Sci* 2004; **31**: 378–82
19 Schmidt BJ, Greenberg CR, Allingham-Hawkins DJ, Spriggs EL. Expression of X-linked bulbospinal muscular atrophy (Kennedy disease) in two homozygous women. *Neurology* 2002; **59**: 770–2
20 Sobue G, Doyu M, Kachi T, Yasuda T, Mukai E, Kumagai T, Mitsuma T. Subclinical phenotypic expressions in heterozygous females of X-linked recessive bulbospinal neuronopathy. *J Neurol Sci* 1993; **117**: 74–8
21 Greenland KJ, Zajac JD. Kennedy's disease: pathogenesis and clinical approaches. *Intern Med J* 2004; **34**: 279–86
22 Mariotti C, Castellotti B, Pareyson D, Testa D, Eoli M, Antozzi C, Silani V, Marconi R, Tezzon F, Siciliano G, Marchini C, Gellera C, Donato SD. Phenotypic manifestations associated with CAG-repeat expansion in the androgen receptor gene in male patients and heterozygous females: a clinical and molecular study of 30 families. *Neuromuscul Disord* 2000; **10**: 391–7
23 Sperfeld AD, Karitzky J, Brummer D, Schreiber H, Haussler J, Ludolph AC, Hanemann CO. X-linked bulbospinal neuronopathy: Kennedy disease. *Arch Neurol* 2002; **59**: 1921–6
24 Poletti A. The polyglutamine tract of androgen receptor: from functions to dysfunctions in motor neurons. *Front Neuroendocrinol* 2004; **25**: 1–26
25 Benten WP, Lieberherr M, Stamm O, Wrehlke C, Guo Z, Wunderlich F. Testosterone signaling through internalizable surface receptors in androgen receptor-free macrophages. *Mol Biol Cell* 1999; **10**: 3113–23
26 Lutz LB, Jamnongjit M, Yang WH, Jahani D, Gill A, Hammes SR. Selective modulation of genomic and nongenomic androgen responses by androgen receptor ligands. *Mol Endocrinol* 2003; **17**: 1106–16
27 Walker WH. Nongenomic actions of androgen in Sertoli cells. *Curr Top Dev Biol* 2003; **56**: 25–53
28 Ntais C, Polycarpou A, Tsatsoulis A. Molecular epidemiology of prostate cancer: androgens and polymorphisms in androgen-related genes. *Eur J Endocrinol* 2003; **149**: 469–77
29 Tanaka F, Doyu M, Ito Y, Matsumoto M, Mitsuma T, Abe K, Aoki M, Itoyama Y, Fischbeck KH, Sobue G. Founder effect in spinal and bulbar muscular atrophy (SBMA). *Hum Mol Genet* 1996; **5**: 1253–7
30 Tanaka F, Reeves MF, Ito Y, Matsumoto M, Li M, Miwa S, Inukai A, Yamamoto M, Doyu M, Yoshida M, Hashizume Y, Terao S, Mitsuma T, Sobue G. Tissue-specific somatic mosaicism in spinal and bulbar muscular atrophy is dependent on CAG-repeat length and androgen receptor – gene expression level. *Am J Hum Genet* 1999; **65**: 966–73
31 La Spada AR, Roling DB, Harding AE, Warner CL, Spiegel R, Hausmanowa-Petrusewicz I, Yee WC, Fischbeck KH. Meiotic stability and genotype-phenotype correlation of the trinucleotide repeat in X-linked spinal and bulbar muscular atrophy. *Nat Genet* 1992; **2**: 301–4

32 Igarashi S, Tanno Y, Onodera O, Yamazaki M, Sato S, Ishikawa A, Miyatani N, Nagashima M, Ishikawa Y, Sahashi K, Ibi T, Miyatake T, Tsuji S. Strong correlation between the number of CAG repeats in androgen receptor genes and the clinical onset of features of spinal and bulbar muscular atrophy. *Neurology* 1992; **42**: 2300–2

33 Doyu M, Sobue G, Mukai E, Kachi T, Yasuda T, Mitsuma T, Takahashi A. Severity of X-linked recessive bulbospinal neuronopathy correlates with size of the tandem CAG repeat in androgen receptor gene. *Ann Neurol* 1992; **32**: 707–10

34 Shimada N, Sobue G, Doyu M, Yamamoto K, Yasuda T, Mukai E, Kachi T, Mitsuma T. X-linked recessive bulbospinal neuronopathy: clinical phenotypes and CAG repeat size in androgen receptor gene. *Muscle Nerve* 1995; **18**: 1378–84

35 Katsuno M, Adachi H, Kume A, Li M, Nakagomi Y, Niwa H, Sang C, Kobayashi Y, Doyu M, Sobue G. Testosterone reduction prevents phenotypic expression in a transgenic mouse model of spinal and bulbar muscular atrophy. *Neuron* 2002; **35**: 843–54

36 Takeyama K, Ito S, Yamamoto A, Tanimoto H, Furutani T, Kanuka H, Miura M, Tabata T, Kato S. Androgen-dependent neurodegeneration by polyglutamine-expanded human androgen receptor in Drosophila. *Neuron* 2002; **35**: 855–64

37 Katsuno M, Adachi H, Doyu M, Minamiyama M, Sang C, Kobayashi Y, Inukai A, Sobue G. Leuprorelin rescues polyglutamine-dependent phenotypes in a transgenic mouse model of spinal and bulbar muscular atrophy. *Nat Med* 2003; **9**: 768–73

38 Sobue G, Matsuoka Y, Mukai E, Takayanagi T, Sobue I, Hashizume Y. Spinal and cranial motor nerve roots in amyotrophic lateral sclerosis and X-linked recessive bulbospinal muscular atrophy: morphometric and teased-fiber study. *Acta Neuropathol (Berl)* 1981; **55**: 227–35

39 Li M, Sobue G, Doyu M, Mukai E, Hashizume Y, Mitsuma T. Primary sensory neurons in X-linked recessive bulbospinal neuropathy: histopathology and androgen receptor gene expression. *Muscle Nerve* 1995; **18**: 301–8

40 Guidetti D, Vescovini E, Motti L, Ghidoni E, Gemignani F, Marbini A, Patrosso MC, Ferlini A, Solime F. X-linked bulbar and spinal muscular atrophy, or Kennedy disease: clinical, neurophysiological, neuropathological, neuropsychological and molecular study of a large family. *J Neurol Sci* 1996; **135**: 140–8

41 Li M, Miwa S, Kobayashi Y, Merry DE, Yamamoto M, Tanaka F, Doyu M, Hashizume Y, Fischbeck KH, Sobue G. Nuclear inclusions of the androgen receptor protein in spinal and bulbar muscular atrophy. *Ann Neurol* 1998; **44**: 249–54

42 Li M, Nakagomi Y, Kobayashi Y, Merry DE, Tanaka F, Doyu M, Mitsuma T, Hashizume Y, Fischbeck KH, Sobue G. Nonneural nuclear inclusions of androgen receptor protein in spinal and bulbar muscular atrophy. *Am J Pathol* 1998; **153**: 695–701

43 Kobayashi Y, Miwa S, Merry DE, Kume A, Mei L, Doyu M, Sobue G. Caspase-3 cleaves the expanded androgen receptor protein of spinal and bulbar muscular atrophy in a polyglutamine repeat length-dependent manner. *Biochem Biophys Res Commun* 1998; **252**: 145–50

44 Ellerby LM, Hackam AS, Propp SS, Ellerby HM, Rabizadeh S, Cashman NR, Trifiro MA, Pinsky L, Wellington CL, Salvesen GS, Hayden MR, Bredesen DE. Kennedy's disease: caspase cleavage of the androgen receptor is a crucial event in cytotoxicity. *J Neurochem* 1999; **72**: 185–95

45 Tanaka M, Machida Y, Nishikawa Y, Akagi T, Hashikawa T, Fujisawa T, Nukina N. Expansion of polyglutamine induces the formation of quasi-aggregate in the early stage of protein fibrillization. *J Biol Chem* 2003; **278**: 34717–24

46 Tanaka M, Morishima I, Akagi T, Hashikawa T, Nukina N. Intra- and intermolecular beta-pleated sheet formation in glutamine-repeat inserted myoglobin as a model for polyglutamine diseases. *J Biol Chem* 2001; **276**: 45470–5

47 Michalik A, Van Broeckhoven C. Pathogenesis of polyglutamine disorders: aggregation revisited. *Hum Mol Genet* 2003; **12**: R173–86

48 Simeoni S, Mancini MA, Stenoien DL, Marcelli M, Weigel NL, Zanisi M, Martini L, Poletti A. Motoneuronal cell death is not correlated with aggregate formation of androgen receptors containing an elongated polyglutamine tract. *Hum Mol Genet* 2000; **9**: 133–44

49 Bates G. Huntingtin aggregation and toxicity in Huntington's disease. *Lancet* 2003; **361**: 1642–4

50 Walcott JL, Merry DE. Trinucleotide repeat disease. The androgen receptor in spinal and bulbar muscular atrophy. *Vitam Horm* 2002; **65**: 127–47

51 Ross CA, Poirier MA, Wanker EE, Amzel M. Polyglutamine fibrillogenesis: the pathway unfolds. *Proc Natl Acad Sci USA* 2003; **100**: 1–3

52 Arrasate M, Mitra S, Schweitzer ES, Segal MR, Finkbeiner S. Inclusion body formation reduces levels of mutant huntingtin and the risk of neuronal death. *Nature* 2004; **431**: 805–10

53 Bowman AB, Yoo SY, Dantuma NP, Zoghbi HY. Neuronal dysfunction in a polyglutamine disease model occurs in the absence of ubiquitin-proteasome system impairment and inversely correlates with the degree of nuclear inclusion formation. *Hum Mol Genet* 2005; **14**: 679–91

54 Rusmini P, Sau D, Crippa V, Palazzolo I, Simonini F, Onesto E, Martini L, Poletti A. Aggregation and proteasome. The case of elongated polyglutamine aggregation in spinal and bulbar muscular atrophy. *Neurobiol Aging* 2006; doi: 10.1016/j.neurobiolaging.2006.05.015

55 Klement IA, Skinner PJ, Kaytor MD, Yi H, Hersch SM, Clark HB, Zoghbi HY, Orr HT. Ataxin-1 nuclear localization and aggregation: role in polyglutamine-induced disease in SCA1 transgenic mice. *Cell* 1998; **95**: 41–53

56 Saudou F, Finkbeiner S, Devys D, Greenberg ME. Huntingtin acts in the nucleus to induce apoptosis but death does not correlate with the formation of intranuclear inclusions. *Cell* 1998; **95**: 55–66

57 Yamada M, Wood JD, Shimohata T, Hayashi S, Tsuji S, Ross CA, Takahashi H. Widespread occurrence of intranuclear atrophin-1 accumulation in the central nervous system neurons of patients with dentatorubral-pallidoluysian atrophy. *Ann Neurol* 2001; **49**: 14–23

58 Adachi H, Katsuno M, Minamiyama M, Waza M, Sang C, Nakagomi Y, Kobayashi Y, Tanaka F, Doyu M, Inukai A, Yoshida M, Hashizume Y, Sobue G. Widespread nuclear and cytoplasmic accumulation of mutant androgen receptor in SBMA patients. *Brain* 2005; **128**: 659–70

59 Sapp E, Schwarz C, Chase K, Bhide PG, Young AB, Penney J, Vonsattel JP, Aronin N, DiFiglia M. Huntingtin localization in brains of normal and Huntington's disease patients. *Ann Neurol* 1997; **42**: 604–12

60 Garden GA, Libby RT, Fu YH, Kinoshita Y, Huang J, Possin DE, Smith AC, Martinez RA, Fine GC, Grote SK, Ware CB, Einum DD, Morrison RS, Ptacek LJ, Sopher BL, La Spada AR. Polyglutamine-expanded ataxin-7 promotes non-cell-autonomous purkinje cell degeneration and displays proteolytic cleavage in ataxic transgenic mice. *J Neurosci* 2002; **22**: 4897–905

61 Watase K, Weeber EJ, Xu B, Antalffy B, Yuva-Paylor L, Hashimoto K, Kano M, Atkinson R, Sun Y, Armstrong DL, Sweatt JD, Orr HT, Paylor R, Zoghbi HY. A long CAG repeat in the mouse Sca1 locus replicates SCA1 features and reveals the impact of protein solubility on selective neurodegeneration. *Neuron* 2002; **34**: 905–19

62 Yoo SY, Pennesi ME, Weeber EJ, Xu B, Atkinson R, Chen S, Armstrong DL, Wu SM, Sweatt JD, Zoghbi HY. SCA7 knockin mice model human SCA7 and reveal gradual accumulation of mutant ataxin-7 in neurons and abnormalities in short-term plasticity. *Neuron* 2003; **37**: 383–401

63 Steffan JS, Kazantsev A, Spasic-Boskovic O, Greenwald M, Zhu YZ, Gohler H, Wanker EE, Bates GP, Housman DE, Thompson LM. The Huntington's disease protein interacts with p53 and CREB-binding protein and represses transcription. *Proc Natl Acad Sci USA* 2000; **97**: 6763–8

64 Nucifora FC Jr, Sasaki M, Peters MF, Huang H, Cooper JK, Yamada M, Takahashi H, Tsuji S, Troncoso J, Dawson VL, Dawson TM, Ross CA. Interference by huntingtin and atrophin-1 with cbp-mediated transcription leading to cellular toxicity. *Science* 2001; **291**: 2423–8

65 Huynh DP, Yang HT, Vakharia H, Nguyen D, Pulst SM. Expansion of the polyQ repeat in ataxin-2 alters its Golgi localization, disrupts the Golgi complex and causes cell death. *Hum Mol Genet* 2003; **12**: 1485–96

66 Yamada M, Tsuji S, Takahashi H. Involvement of lysosomes in the pathogenesis of CAG repeat diseases. *Ann Neurol* 2002; **52**: 498–503

67 Taylor JP, Tanaka F, Robitschek J, Sandoval CM, Taye A, Markovic-Plese S, Fischbeck KH. Aggresomes protect cells by enhancing the degradation of toxic polyglutamine-containing protein. *Hum Mol Genet* 2003; **12**: 749–57

68 Ravikumar B, Duden R, Rubinsztein DC. Aggregate-prone proteins with polyglutamine and polyalanine expansions are degraded by autophagy. *Hum Mol Genet* 2002; **11**: 1107–17

69 Kegel KB, Kim M, Sapp E, McIntyre C, Castano JG, Aronin N, DiFiglia M. Huntingtin expression stimulates endosomal-lysosomal activity, endosome tubulation, and autophagy. *J Neurosci* 2000; **20**: 7268–78

70 Ishisaka R, Utsumi T, Yabuki M, Kanno T, Furuno T, Inoue M, Utsumi K. Activation of caspase-3-like protease by digitonin-treated lysosomes. *FEBS Lett* 1998; **435**: 233–6

71 Gatchel JR, Zoghbi HY. Diseases of unstable repeat expansion: mechanisms and common principles. *Nat Rev Genet* 2005; **6**: 743–55

72 Yeh S, Tsai MY, Xu Q, Mu XM, Lardy H, Huang KE, Lin H, Yeh SD, Altuwaijri S, Zhou X, Xing L, Boyce BF, Hung MC, Zhang S, Gan L, Chang C. Generation and characterization of androgen receptor knockout (ARKO) mice: an in vivo model for the study of androgen functions in selective tissues. *Proc Natl Acad Sci USA* 2002; **99**: 13498–503

73 Adachi H, Kume A, Li M, Nakagomi Y, Niwa H, Do J, Sang C, Kobayashi Y, Doyu M, Sobue G. Transgenic mice with an expanded CAG repeat controlled by the human AR promoter show polyglutamine nuclear inclusions and neuronal dysfunction without neuronal cell death. *Hum Mol Genet* 2001; **10**: 1039–48

74 Yu Z, Dadgar N, Albertelli M, Scheller A, Albin RL, Robins DM, Lieberman AP. Abnormalities of germ cell maturation and sertoli cell cytoskeleton in androgen receptor 113 CAG knock-in mice reveal toxic effects of the mutant protein. *Am J Pathol* 2006; **168**: 195–204

75 Thomas PS Jr, Fraley GS, Damien V, Woodke LB, Zapata F, Sopher BL, Plymate SR, La Spada AR. Loss of endogenous androgen receptor protein accelerates motor neuron degeneration and accentuates androgen insensitivity in a mouse model of X-linked spinal and bulbar muscular atrophy. *Hum Mol Genet* 2006; **15**: 2225–38

76 Kemppainen JA, Lane MV, Sar M, Wilson EM. Androgen receptor phosphorylation, turnover, nuclear transport, and transcriptional activation. Specificity for steroids and antihormones. *J Biol Chem* 1992; **267**: 968–74

77 Lieberman AP, Harmison G, Strand AD, Olson JM, Fischbeck KH. Altered transcriptional regulation in cells expressing the expanded polyglutamine androgen receptor. *Hum Mol Genet* 2002; **11**: 1967–76

78 Merry DE. Animal models of Kennedy disease. *Neurorx* 2005; **2**: 471–9

79 Chevalier-Larsen ES, O'Brien CJ, Wang H, Jenkins SC, Holder L, Lieberman AP, Merry DE. Castration restores

function and neurofilament alterations of aged symptomatic males in a transgenic mouse model of spinal and bulbar muscular atrophy. *J Neurosci* 2004; **24**: 4778–86

80 Banno H, Adachi H, Katsuno M, Suzuki K, Atsuta N, Watanabe H, Tanaka F, Doyu M, Sobue G. Mutant androgen receptor accumulation in spinal and bulbar muscular atrophy scrotal skin: a pathogenic marker. *Ann Neurol* 2006; **59**: 520–6

81 Fang Y, Fliss AE, Robins DM, Caplan AJ. Hsp90 regulates androgen receptor hormone binding affinity in vivo. *J Biol Chem* 1996; **271**: 28697–702

82 Georget V, Terouanne B, Nicolas JC, Sultan C. Mechanism of antiandrogen action: key role of hsp90 in conformational change and transcriptional activity of the androgen receptor. *Biochemistry* 2002; **41**: 11824–31

83 Pratt WB, Toft DO. Regulation of signaling protein function and trafficking by the hsp90/hsp70-based chaperone machinery. *Exp Biol Med (Maywood)* 2003; **228**: 111–33

84 Sullivan W, Stensgard B, Caucutt G, Bartha B, McMahon N, Alnemri ES, Litwack G, Toft D. Nucleotides and two functional states of hsp90. *J Biol Chem* 1997; **272**: 8007–12

85 Neckers L. Heat shock protein 90 inhibition by 17-allylamino-17-demethoxygeldanamycin: a novel therapeutic approach for treating hormone-refractory prostate cancer. *Clin Cancer Res* 2002; **8**: 962–6

86 Egorin MJ, Zuhowski EG, Rosen DM, Sentz DL, Covey JM, Eiseman JL. Plasma pharmacokinetics and tissue distribution of 17-(allylamino)-17-demethoxygeldanamycin (NSC 330507) in CD2F1 mice1. *Cancer Chemother Pharmacol* 2001; **47**: 291–302

87 McClellan AJ, Scott MD, Frydman J. Folding and quality control of the VHL tumor suppressor proceed through distinct chaperone pathways. *Cell* 2005; **121**: 739–48

88 Felts SJ, Toft DO. p23, a simple protein with complex activities. *Cell Stress Chaperones* 2003; **8**: 108–13

89 Mimnaugh EG, Chavany C, Neckers L. Polyubiquitination and proteasomal degradation of the p185c-erbB-2 receptor protein-tyrosine kinase induced by geldanamycin. *J Biol Chem* 1996; **271**: 22796–801

90 Bonvini P, Dalla Rosa H, Vignes N, Rosolen A. Ubiquitination and proteasomal degradation of nucleophosmin-anaplastic lymphoma kinase induced by 17-allylamino-demethoxygeldanamycin: role of the co-chaperone carboxyl heat shock protein 70-interacting protein. *Cancer Res* 2004; **64**: 3256–64

91 Smith DF, Whitesell L, Nair SC, Chen S, Prapapanich V, Rimerman RA. Progesterone receptor structure and function altered by geldanamycin, an hsp90-binding agent. *Mol Cell Biol* 1995; **15**: 6804–12

92 Johnson JL, Toft DO. Binding of p23 and hsp90 during assembly with the progesterone receptor. *Mol Endocrinol* 1995; **9**: 670–8

93 Vanaja DK, Mitchell SH, Toft DO, Young CY. Effect of geldanamycin on androgen receptor function and stability. *Cell Stress Chaperones* 2002; **7**: 55–64

94 Solit DB, Zheng FF, Drobnjak M, Munster PN, Higgins B, Verbel D, Heller G, Tong W, Cordon-Cardo C, Agus DB, Scher HI, Rosen N. 17-Allylamino-17-demethoxygeldanamycin induces the degradation of androgen receptor and HER-2/neu and inhibits the growth of prostate cancer xenografts. *Clin Cancer Res* 2002; **8**: 986–93

95 Neckers L. Hsp90 inhibitors as novel cancer chemotherapeutic agents. *Trends Mol Med* 2002; **8**: S55–61

96 Xiao N, Callaway CW, Lipinski CA, Hicks SD, DeFranco DB. Geldanamycin provides posttreatment protection against glutamate-induced oxidative toxicity in a mouse hippocampal cell line. *J Neurochem* 1999; **72**: 95–101

97 Sano M. Radicicol and geldanamycin prevent neurotoxic effects of anti-cancer drugs on cultured embryonic sensory neurons. *Neuropharmacology* 2001; **40**: 947–53

98 Xu L, Ouyang YB, Giffard RG. Geldanamycin reduces necrotic and apoptotic injury due to oxygen-glucose deprivation in astrocytes. *Neurol Res* 2003; **25**: 697–700

99 Ouyang YB, Xu L, Giffard RG. Geldanamycin treatment reduces delayed CA1 damage in mouse hippocampal organotypic cultures subjected to oxygen glucose deprivation. *Neurosci Lett* 2005; **380**: 229–33

100 Waza M, Adachi H, Katsuno M, Minamiyama M, Sang C, Tanaka F, Inukai A, Doyu M, Sobue G. 17-AAG, an Hsp90 inhibitor, ameliorates polyglutamine-mediated motor neuron degeneration. *Nat Med* 2005; **11**: 1088–95

101 Sittler A, Lurz R, Lueder G, Priller J, Lehrach H, Hayer-Hartl MK, Hartl FU, Wanker EE. Geldanamycin activates a heat shock response and inhibits huntingtin aggregation in a cell culture model of Huntington's disease. *Hum Mol Genet* 2001; **10**: 1307–15

102 Harrell JM, Murphy PJ, Morishima Y, Chen H, Mansfield JF, Galigniana MD, Pratt WB. Evidence for glucocorticoid receptor transport on microtubules by dynein. *J Biol Chem* 2004; **279**: 54647–54

103 Wochnik GM, Ruegg J, Abel GA, Schmidt U, Holsboer F, Rein T. FK506-binding proteins 51 and 52 differentially regulate dynein interaction and nuclear translocation of the glucocorticoid receptor in mammalian cells. *J Biol Chem* 2005; **280**: 4609–16

104 Thomas M, Harrell JM, Morishima Y, Peng HM, Pratt WB, Lieberman AP. Pharmacologic and genetic inhibition of hsp90-dependent trafficking reduces aggregation and promotes degradation of the expanded glutamine androgen receptor without stress protein induction. *Hum Mol Genet* 2006; **15**: 1876–83

105 Adachi H, Katsuno M, Minamiyama M, Sang C, Pagoulatos G, Angelidis C, Kusakabe M, Yoshiki A, Kobayashi Y, Doyu M, Sobue G. Heat shock protein 70 chaperone

overexpression ameliorates phenotypes of the spinal and bulbar muscular atrophy transgenic mouse model by reducing nuclear-localized mutant androgen receptor protein. *J Neurosci* 2003; **23**: 2203–11

106 Minamiyama M, Katsuno M, Adachi H, Waza M, Sang C, Kobayashi Y, Tanaka F, Doyu M, Inukai A, Sobue G. Sodium butyrate ameliorates phenotypic expression in a transgenic mouse model of spinal and bulbar muscular atrophy. *Hum Mol Genet* 2004; **13**: 1183–92

107 Whitesell L, Bagatell R, Falsey R. The stress response: implications for the clinical development of hsp90 inhibitors. *Curr Cancer Drug Targets* 2003; **3**: 349–58

108 Kamal A, Boehm MF, Burrows FJ. Therapeutic and diagnostic implications of Hsp90 activation. *Trends Mol Med* 2004; **10**: 283–90

109 Muchowski PJ, Wacker JL. Modulation of neurodegeneration by molecular chaperones. *Nat Rev Neurosci* 2005; **6**: 11–22

110 Xia H, Mao Q, Eliason SL, Harper SQ, Martins IH, Orr HT, Paulson HL, Yang L, Kotin RM, Davidson BL. RNAi suppresses polyglutamine-induced neurodegeneration in a model of spinocerebellar ataxia. *Nat Med* 2004; **10**: 816–20

111 Harper SQ, Staber PD, He X, Eliason SL, Martins IH, Mao Q, Yang L, Kotin RM, Paulson HL, Davidson BL. RNA interference improves motor and neuropathological abnormalities in a Huntington's disease mouse model. *Proc Natl Acad Sci USA* 2005; **102**: 5820–5

112 Raoul C, Abbas-Terki T, Bensadoun JC, Guillot S, Haase G, Szulc J, Henderson CE, Aebischer P. Lentiviral-mediated silencing of SOD1 through RNA interference retards disease onset and progression in a mouse model of ALS. *Nat Med* 2005; **11**: 423–8

113 La Spada AR, Weydt P. Targeting toxic proteins for turnover. *Nat Med* 2005; **11**: 1052–3

114 Cummings CJ, Mancini MA, Antalffy B, DeFranco DB, Orr HT, Zoghbi HY. Chaperone suppression of aggregation and altered subcellular proteasome localization imply protein misfolding in SCA1. *Nat Genet* 1998; **19**: 148–54

115 Ciechanover A, Brundin P. The ubiquitin proteasome system in neurodegenerative diseases: sometimes the chicken, sometimes the egg. *Neuron* 2003; **40**: 427–46

116 Bence NF, Sampat RM, Kopito RR. Impairment of the ubiquitin-proteasome system by protein aggregation. *Science* 2001; **292**: 1552–5

117 Jana NR, Zemskov EA, Wang G, Nukina N. Altered proteasomal function due to the expression of polyglutamine-expanded truncated N-terminal huntingtin induces apoptosis by caspase activation through mitochondrial cytochrome c release. *Hum Mol Genet* 2001; **10**: 1049–59

118 Holmberg CI, Staniszewski KE, Mensah KN, Matouschek A, Morimoto RI. Inefficient degradation of truncated polyglutamine proteins by the proteasome. *EMBO J* 2004; **23**: 4307–18

119 Zhou H, Cao F, Wang Z, Yu ZX, Nguyen HP, Evans J, Li SH, Li XJ. Huntingtin forms toxic NH2-terminal fragment complexes that are promoted by the age-dependent decrease in proteasome activity. *J Cell Biol* 2003; **163**: 109–18

120 Bett JS, Goellner GM, Woodman B, Pratt G, Rechsteiner M, Bates GP. Proteasome impairment does not contribute to pathogenesis in R6/2 Huntington's disease mice: exclusion of proteasome activator REG{gamma} as a therapeutic target. *Hum Mol Genet* 2006; **15**: 33–44

121 Yamamoto A, Lucas JJ, Hen R. Reversal of neuropathology and motor dysfunction in a conditional model of Huntington's disease. *Cell* 2000; **101**: 57–66

122 Zu T, Duvick LA, Kaytor MD, Berlinger MS, Zoghbi HY, Clark HB, Orr HT. Recovery from polyglutamine-induced neurodegeneration in conditional SCA1 transgenic mice. *J Neurosci* 2004; **24**: 8853–61

123 Macario AJ, Conway de Macario E. Sick chaperones, cellular stress, and disease. *N Engl J Med* 2005; **353**: 1489–501

124 Heinlein CA, Chang C. Role of chaperones in nuclear translocation and transactivation of steroid receptors. *Endocrine* 2001; **14**: 143–9

125 Rokutan K, Hirakawa T, Teshima S, Nakano Y, Miyoshi M, Kawai T, Konda E, Morinaga H, Nikawa T, Kishi K. Implications of heat shock/stress proteins for medicine and disease. *J Med Invest* 1998; **44**: 137–47

126 Warrick JM, Chan HY, Gray-Board GL, Chai Y, Paulson HL, Bonini NM. Suppression of polyglutamine-mediated neurodegeneration in Drosophila by the molecular chaperone HSP70. *Nat Genet* 1999; **23**: 425–8

127 Wyttenbach A, Carmichael J, Swartz J, Furlong RA, Narain Y, Rankin J, Rubinsztein DC. Effects of heat shock, heat shock protein 40 (HDJ-2), and proteasome inhibition on protein aggregation in cellular models of Huntington's disease. *Proc Natl Acad Sci USA* 2000; **97**: 2898–903

128 Wyttenbach A. Role of heat shock proteins during polyglutamine neurodegeneration: mechanisms and hypothesis. *J Mol Neurosci* 2004; **23**: 69–96

129 Kobayashi Y, Kume A, Li M, Doyu M, Hata M, Ohtsuka K, Sobue G. Chaperones Hsp70 and Hsp40 suppress aggregate formation and apoptosis in cultured neuronal cells expressing truncated androgen receptor protein with expanded polyglutamine tract. *J Biol Chem* 2000; **275**: 8772–8

130 Bailey CK, Andriola IF, Kampinga HH, Merry DE. Molecular chaperones enhance the degradation of expanded polyglutamine repeat androgen receptor in a cellular model of spinal and bulbar muscular atrophy. *Hum Mol Genet* 2002; **11**: 515–23

131 Cummings CJ, Sun Y, Opal P, Antalffy B, Mestril R, Orr HT, Dillmann WH, Zoghbi HY. Over-expression of inducible HSP70 chaperone suppresses neuropathology and improves motor function in SCA1 mice. *Hum Mol Genet* 2001; **10**: 1511–18

132 Hay DG, Sathasivam K, Tobaben S, Stahl B, Marber M, Mestril R, Mahal A, Smith DL, Woodman B, Bates GP. Progressive decrease in chaperone protein levels in a mouse model of Huntington's disease and induction of stress proteins as a therapeutic approach. *Hum Mol Genet* 2004; **13**: 1389–405

133 Agrawal N, Pallos J, Slepko N, Apostol BL, Bodai L, Chang LW, Chiang AS, Thompson LM, Marsh JL. Identification of combinatorial drug regimens for treatment of Huntington's disease using Drosophila. *Proc Natl Acad Sci USA* 2005; **102**: 3777–81

134 Dou F, Netzer WJ, Tanemura K, Li F, Hartl FU, Takashima A, Gouras GK, Greengard P, Xu H. Chaperones increase association of tau protein with microtubules. *Proc Natl Acad Sci USA* 2003; **100**: 721–6

135 Petrucelli L, Dickson D, Kehoe K, Taylor J, Snyder H, Grover A, De Lucia M, McGowan E, Lewis J, Prihar G, Kim J, Dillmann WH, Browne SE, Hall A, Voellmy R, Tsuboi Y, Dawson TM, Wolozin B, Hardy J, Hutton M. CHIP and Hsp70 regulate tau ubiquitination, degradation and aggregation. *Hum Mol Genet* 2004; **13**: 703–14

136 Benussi L, Ghidoni R, Paterlini A, Nicosia F, Alberici AC, Signorini S, Barbiero L, Binetti G. Interaction between tau and alpha-synuclein proteins is impaired in the presence of P301L tau mutation. *Exp Cell Res* 2005; **308**: 78–84

137 Auluck PK, Bonini NM. Pharmacological prevention of Parkinson disease in Drosophila. *Nat Med* 2002; **8**: 1185–6

138 Auluck PK, Meulener MC, Bonini NM. Mechanisms of suppression of {alpha}-synuclein neurotoxicity by geldanamycin in Drosophila. *J Biol Chem* 2005; **280**: 2873–8

139 Flower TR, Chesnokova LS, Froelich CA, Dixon C, Witt SN. Heat shock prevents alpha-synuclein-induced apoptosis in a yeast model of Parkinson's disease. *J Mol Biol* 2005; **351**: 1081–100

140 Lu A, Ran R, Parmentier-Batteur S, Nee A, Sharp FR. Geldanamycin induces heat shock proteins in brain and protects against focal cerebral ischemia. *J Neurochem* 2002; **81**: 355–64

141 Giffard RG, Xu L, Zhao H, Carrico W, Ouyang Y, Qiao Y, Sapolsky R, Steinberg G, Hu B, Yenari MA. Chaperones, protein aggregation, and brain protection from hypoxic/ischemic injury. *J Exp Biol* 2004; **207**: 3213–20

142 Murphy P, Sharp A, Shin J, Gavrilyuk V, Dello Russo C, Weinberg G, Sharp FR, Lu A, Heneka MT, Feinstein DL. Suppressive effects of ansamycins on inducible nitric oxide synthase expression and the development of experimental autoimmune encephalomyelitis. *J Neurosci Res* 2002; **67**: 461–70

143 Hirakawa T, Rokutan K, Nikawa T, Kishi K. Geranylgeranylacetone induces heat shock proteins in cultured guinea pig gastric mucosal cells and rat gastric mucosa. *Gastroenterology* 1996; **111**: 345–57

144 Katsuno M, Sang C, Adachi H, Minamiyama M, Waza M, Tanaka F, Doyu M, Sobue G. Pharmacological induction of heat-shock proteins alleviates polyglutamine-mediated motor neuron disease. *Proc Natl Acad Sci USA* 2005; **102**: 16801–6

145 Cowan KJ, Diamond MI, Welch WJ. Polyglutamine protein aggregation and toxicity are linked to the cellular stress response. *Hum Mol Genet* 2003; **12**: 1377–91

146 Batulan Z, Shinder GA, Minotti S, He BP, Doroudchi MM, Nalbantoglu J, Strong MJ, Durham HD. High threshold for induction of the stress response in motor neurons is associated with failure to activate HSF1. *J Neurosci* 2003; **23**: 5789–98

Received 29 August 2006
Accepted after revision 18 December 2006

ELSEVIER

Neurobiology of Disease

www.elsevier.com/locate/ynbdi
Neurobiology of Disease 25 (2007) 331–341

Dorfin-CHIP chimeric proteins potently ubiquitylate and degrade familial ALS-related mutant SOD1 proteins and reduce their cellular toxicity

Shinsuke Ishigaki,[a,b] Jun-ichi Niwa,[a] Shin-ichi Yamada,[a] Miho Takahashi,[a] Takashi Ito,[a] Jun Sone,[a] Manabu Doyu,[a] Fumihiko Urano,[b,c] and Gen Sobue[a,*]

[a]*Department of Neurology, Nagoya University Graduate School of Medicine, Nagoya 466-8500, Japan*
[b]*Program in Gene Function and Expression, University of Massachusetts Medical School, Worcester, MA 01605, USA*
[c]*Program in Molecular Medicine, University of Massachusetts Medical School, Worcester, MA 01605, USA*

Received 19 May 2006; revised 8 September 2006; accepted 22 September 2006
Available online 6 December 2006

The ubiquitin–proteasome system (UPS) is involved in the pathogenetic mechanisms of neurodegenerative disorders, including amyotrophic lateral sclerosis (ALS). Dorfin is a ubiquitin ligase (E3) that degrades mutant SOD1 proteins, which are responsible for familial ALS. Although Dorfin has potential as an anti-ALS molecule, its life in cells is short. To improve its stability and enhance its E3 activity, we developed chimeric proteins containing the substrate-binding hydrophobic portion of Dorfin and the U-box domain of the carboxyl terminus of Hsc70-interacting protein (CHIP), which has strong E3 activity through the U-box domain. All the Dorfin-CHIP chimeric proteins were more stable in cells than was wild-type Dorfin ($Dorfin^{WT}$). One of the Dorfin-CHIP chimeric proteins, $Dorfin\text{-}CHIP^{L}$, ubiquitylated mutant SOD1 more effectively than did $Dorfin^{WT}$ and CHIP *in vivo*, and degraded mutant SOD1 protein more rapidly than $Dorfin^{WT}$ does. Furthermore, $Dorfin\text{-}CHIP^{L}$ rescued neuronal cells from mutant SOD1-associated toxicity and reduced the aggresome formation induced by mutant SOD1 more effectively than did $Dorfin^{WT}$.

Keywords: Dorfin; ALS; SOD1; CHIP; Neurodegeneration; Ubiquitin–proteasome system

Amyotrophic lateral sclerosis (ALS), one of the most common neurodegenerative disorders, is characterized by selective motor neuron degeneration in the spinal cord, brainstem, and cortex. About 10% of ALS cases are familial; of these, 10%–20% are caused by Cu/Zn superoxide dismutase (SOD1) gene mutations (Rosen et al., 1993; Cudkowicz et al., 1997). However, the precise mechanism that causes motor neuron death in ALS is still unknown, although many have been proposed: oxidative toxicity, glutamate receptor abnormality, ubiquitin proteasome dysfunction, inflammatory and cytokine activation, neurotrophic factor deficiency, mitochondrial damage, cytoskeletal abnormalities, and activation of the apoptosis pathway (Julien, 2001; Rowland and Shneider, 2001).

Misfolded protein accumulation, one probable cause of neurodegenerative disorders, including ALS, can cause the deterioration of various cellular functions, leading to neuronal cell death (Julien, 2001; Ciechanover and Brundin, 2003). Recent findings indicate that the ubiquitin–proteasome system (UPS), a cellular function that recognizes and catalyzes misfolded or impaired cellular proteins (Jungmann et al., 1993; Lee et al., 1996; Bercovich et al., 1997), is involved in the pathogenesis of various neurodegenerative diseases, among them ALS, Parkinson's disease (PD), Alzheimer's disease, polyglutamine disease, and prion disease (Alves-Rodrigues et al., 1998; Sherman and Goldberg, 2001; Ciechanover and Brundin, 2003). The ubiquitin ligase (E3), a key molecule for the UPS, can specifically recognize misfolded substrates and convey them to proteasomal degradation (Scheffner et al., 1995; Glickman and Ciechanover, 2002; Tanaka et al., 2004).

Dorfin, an E3 protein, contains an in-between-ring-finger (RING-IBR) domain at its N-terminus. The C-terminus of Dorfin can recognize mutant SOD1 proteins, which cause familial ALS (Niwa et al., 2001; Ishigaki et al., 2002b; Niwa et al., 2002). In cultured cells, Dorfin colocalized with aggresomes and ubiquitin-positive inclusions, which are pathological hallmarks of neurodegenerative diseases (Hishikawa et al., 2003; Ito et al., 2003). Dorfin also interacted with VCP/p97 in ubiquitin-positive inclusions in

Abbreviations: ALS, amyotrophic lateral sclerosis; CFTR, cystic fibrosis transmembrane conductance regulator; CHIP, carboxyl terminus of Hsc70-interacting protein; DMEM, Dulbecco's modified Eagle's medium; E3, ubiquitin ligase; FCS, fetal calf serum; IP, immunoprecipitation; LB, Lewy body; PD, Parkinson's disease; RING-IBR, in-between-ring-finger; SCF, Skp1-Cullin-F box complex; SDS-PAGE, sodium dodecyl sulfate-polyacrylamide gel electrophoresis; SOD1, Cu/Zn super oxide dismutase; UPS, ubiquitin–proteasome system.

* Corresponding author. Fax: +81 52 744 2384.
E-mail address: sobueg@med.nagoya-u.ac.jp (G. Sobue).
Available online on ScienceDirect (www.sciencedirect.com).

0969-9961/$ - see front matter © 2006 Elsevier Inc. All rights reserved.
doi:10.1016/j.nbd.2006.09.017

ALS and PD (Ishigaki et al., 2004). Moreover, formation of this complex was found to be necessary for the E3 activity of Dorfin against mutant SOD1. These findings suggest that Dorfin is involved in the quality-control system for the abnormal proteins that accumulate in the affected neurons in neurodegenerative disorders.

Dorfin degrades mutant SOD1s and attenuates mutant SOD1-associated toxicity in cultured cells (Niwa et al., 2002). However, in Dorfin/mutant SOD1 double transgenic mice, we found only a modest beneficial effect on mutant SOD1-induced survival and motor dysfunction (unpublished data). These findings, combined with the short half-life of Dorfin protein, led us to hypothesize that the limiting effect of the Dorfin transgene may be a consequence of autodegradation of Dorfin, since Dorfin can execute autoubiquitilation *in vivo* (Niwa et al., 2001).

Carboxyl terminus of Hsc70-interacting protein (CHIP) is also an E3 protein; it has a TPR domain in the N terminus and a U-box domain in the C terminus. The U-box domain of CHIP is responsible for its strong E3 activity, whereas the TPR domain recruits heat shock proteins harboring misfolded client proteins such as cystic fibrosis transmembrane conductance regulator (CFTR), denatured luciferase, and tau (Meacham et al., 2001; Murata et al., 2001, 2003; Hatakeyama et al., 2004; Shimura et al., 2004).

To prolong the protein lifetime of Dorfin and thereby obtain more potent ubiquitylation and degradation activity against mutant SOD1s than is provided by Dorfin or CHIP alone, we generated chimeric proteins containing the substrate-binding domain of Dorfin and the UPR domain of CHIP substitute for RING/IBR of Dorfin. We developed 12 candidate constructs that encode Dorfin-CHIP chimeric proteins and analyzed them for their E3 activities and degradation abilities against mutant SOD1 protein in cultured cells.

Experimental procedures

Plasmids and antibodies

We designed constructs expressing Dorfin-CHIP chimeric protein. In these constructs, different-length fragments of the C-terminus portion of Dorfin, including the hydrophobic substrate-binding domain (amino acids 333–838, 333–700, and 333–454) and the C-terminus UPR domain of CHIP with amino acids 128–303 or without amino acids 201–303, a charged region was fused in various combinations as shown in Fig. 2C. Briefly, Dorfin-CHIP$^{A, B, C, G, H,}$ and ^{I} had the C-terminus portion of Dorfin in their N-terminus and the U-box of CHIP in their C-terminus; Dorfin-CHIP$^{D, E, F, J, K,}$ and ^{L} had the U-box of CHIP in their N-terminus and the C-terminus portion of Dorfin in their C-terminus.

We prepared a pCMV2/FLAG-Dorfin-CHIP chimeric vector (Dorfin-CHIP) by polymerase chain reaction (PCR) using the appropriate design of PCR primers with restriction sites (*Cla*I, *Kpn*I, and *XBa*I or *Eco*RI, *Cla*I, and *Kpn*I). The PCR products were digested and inserted into the *Cla*I–*Kpn*I site in pCMV2 vector (Sigma, St. Louis, MO). These vectors have been described previously: pFLAG-Dorfin^{WT} (Dorfin^{WT}), FLAG-Dorfin$^{C132S/C135S}$ (Dorfin$^{C132S/C135S}$), pFLAG-CHIP (CHIP), pFLAG-Mock (Mock), pcDNA3.1/Myc-SOD1^{WT} (SOD1^{WT}), pcDNA3.1/Myc-SOD1^{G93A} (SOD1^{G93A}), pcDNA3.1/Myc-SOD1^{G85R} (SOD1^{G85R}), pcDNA3.1/Myc-SOD1^{H46R} (SOD1^{H46R}), pcDNA3.1/Myc-SOD1^{G37R} (SOD1^{G37R}), pEGFP/SOD1^{WT} (SOD1^{WT}-GFP), and pEGFP/SOD1^{G85R} (SOD1^{G85R}-GFP) (Ishigaki et al., 2004). We used monoclonal anti-FLAG antibody (M2; Sigma), monoclonal anti-Myc antibody (9E10; Santa Cruz Biotechnology, Santa Cruz, CA), monoclonal anti-HA antibody (12CA5; Roche, Basel, Switzerland), and polyclonal anti-SOD1 (SOD-100; Stressgen, San Diego, CA).

Cell culture and transfection

We grew HEK293 cells and neuro2a (N2a) cells in Dulbecco's modified Eagle's medium (DMEM) containing 10% fetal calf serum (FCS), 5 U/ml penicillin, and 50 μg/ml streptomycin. At subconfluence, we transfected these cells with the indicated plasmids, using Effectene reagent (Qiagen, Valencia, CA) for HEK293 cells and Lipofectamine 2000 (Invitrogen, Carlsbad, CA) for N2a cells. After overnight posttransfection, we treated the cells with 1 μM MG132 (Z-Leu-Leu-Leu-al; Sigma) for 16 h to inhibit cellular proteasome activity. We analyzed the cells 24–48 h after transfection. To differentiate N2a cells, cells were treated for 48 h with 15 μM of retinoic acid in 2% serum medium.

Immunological analysis

At 24–48 h after transfection, we lysed cells (4×10^5 in 6-cm dishes) with 500 μl of lysis buffer consisting of 50 mM Tris–HCl, 150 mM NaCl, 1% Nonidet P-40, and 1 mM ethylenediaminetetraacetic acid (EDTA), as well as a protease inhibitor cocktail (Complete Mini, Roche). The lysate was then centrifuged at $10{,}000 \times g$ for 10 min at 4°C to remove debris. We used a 10% volume of the supernatants as the lysate for SDS-PAGE. When immunoprecipitated, the supernatants were precleared with protein A/G agarose (Santa-Cruz). A specific antibody, either anti-FLAG (M2) or anti-Myc (9E10), was then added. We incubated the immune complexes, first at 4°C with rotation and with protein A/G agarose (Roche) for 3 h, after which they were collected by centrifugation and washed four times with the lysis buffer. For protein analysis, immune complexes were dissociated by heating in SDS-PAGE sample buffer and loaded onto SDS-PAGE. We separated the samples by SDS-PAGE (15% gel or 5%–20% gradient gel) and transferred them onto polyvinylidene difluoride membranes. We then immunoblotted samples with specific antibodies.

Immunohistochemistry

We fixed differentiated N2a cells grown in plastic dishes in 4% paraformaldehyde in PBS for 15 min. The cells were then blocked for 30 min with 5% (vol/vol) normal goat serum in PBS, incubated overnight at 4°C with anti-FLAG antibody (M2), washed with PBS, and incubated for 30 min with Alexa 496 nm anti-mouse antibodies (Molecular Probes, Eugene, OR). We mounted the cells on slides and obtained images using a fluorescence microscope (IX71; Olympus, Tokyo, Japan) equipped with a cooled charge-coupled device camera (DP70; Olympus). Photographs were taken using DP Controller software (Olympus).

Analysis of protein stability

We assayed the stability of proteins by pulse-chase analysis using [^{35}S] followed by immunoprecipitation. Metabolic labeling was performed as described previously (Yoshida et al., 2003). Briefly, in the pulse-chase analysis of Dorfin proteins, HEK293 cells in 6-cm dishes were transiently transfected with 1 μg of

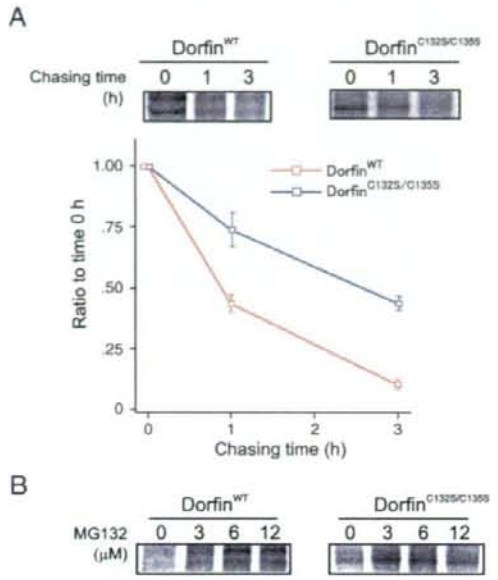

Fig. 1. Pulse-chase analysis of Dorfin^{WT} and Dorfin$^{C132S/C135S}$. (A) Dorfin^{WT} or Dorfin$^{C132S/C135S}$ was overexpressed in HEK293 cells. After overnight incubation, [^{35}S]-labeled Met/Cys pulse-chase analysis was performed. Cells were harvested and analyzed at 0, 1, or 3 h after labeling and immunoprecipitation by anti-FLAG antibody (upper panels). To determine serial changes in the amount of Dorfin^{WT} or Dorfin$^{C132S/C135S}$, four independent experiments were performed and the amounts of Dorfin^{WT} and Dorfin$^{C132S/C135S}$ were plotted. The differences between the amounts of Dorfin^{WT} and Dorfin$^{C132S/C135S}$ were significant at 1 h ($p<0.01$) and 3 h after labeling ($p<0.001$) (lower panels). Values are the means ± SE, $n=4$. Statistics were done using an unpaired t-test. (B) Cells overexpressing Dorfin^{WT} or Dorfin$^{C132S/C135S}$ were treated with different concentrations of MG132 for 3 h after labeling.

FLAG-Dorfin^{WT} or FLAG-Dorfin$^{C132S/C135S}$. In pulse-chase experiments using SOD1^{G85R}, N2a cells in 6-cm dishes were transiently transfected with 1 μg of SOD1^{G85R}-Myc or SOD1^{G93A}-Myc and FLAG-Mock, FLAG-Dorfin, or FLAG-Dorfin-CHIP^{L}. FLAG-Mock was used as a negative control. After starving the cells for 60 min in methionine- and cysteine-free DMEM with 10% FCS, we labeled them for 60 min with 150 μCi/ml of Pro-Mix L-[^{35}S] *in vitro* cell-labeling mix (Amersham Biosciences). Cells were chased for different lengths of time at 37°C. In experiments with proteasomal inhibition, we added different amounts of MG132 in medium during the chase period. We performed immunoprecipitation using protein A/G agarose, mouse monoclonal anti-FLAG (M2), and anti-Myc (9E10). The intensity of the bands was quantified by ImageGauge software (Fuji Film, Tokyo, Japan).

MTS assay

We transfected N2a cells (5000 cells per well) in 96-well collagen-coated plates with 0.15 μg of SOD1^{G85R}-GFP and 0.05 μg of Dorfin, CHIP, Dorfin-CHIP^{L}, or pCMV2 vector (Mock) using Effecten reagent (Qiagen). Then we performed 3-(4,5-dimethylthiazol-2-yl)-5-(3-carboxymethoxyphenyl)-2-(4-sulfophenyl)-2*H*-tetrazolium inner salt (MTS) assays using Cell Titer 96 (Promega) at 48 h after incubation. This procedure has previously been described (Ishigaki et al., 2002a).

Aggregation assay

We transfected N2a cells in 6-cm dishes with 1.0 μg of SOD1^{G85R}-GFP and 1.0 μg of FLAG-Mock, FLAG-Dorfin, FLAG-CHIP, or FLAG-Dorfin-CHIP^{L}. After overnight incubation, we changed the medium to 2% FCS containing medium with 15 μM retinoic acid (RA) for differentiation. In the MG132 (+) group, 1 μM of MG132 was added after 24 h of differentiation stimuli. After 48 h of differentiation stimuli, we examined the cells in their living condition by fluorescence microscopy. The transfection ratio was equivalent (75%) among all groups. Visually observable macro aggregation-harboring cells were counted as "aggregation positive" cells (Fig. 7C). All cells were counted in fields selected at random from the four different quadrants of the culture dish. Counting was done by an investigator who was blind to the experimental condition.

Results

Dorfin degradation by the UPS in vivo

We analyzed the degradation speed of FLAG-Dorfin by the pulse-chase method using [^{35}S] labeling, finding that more than half of wild-type Dorfin (Dorfin^{WT}) was degraded within 1 h (Fig. 1A). This degradation was dose-dependently inhibited by MG132, a proteasome inhibitor (Fig. 1B). On the other hand, the RING mutant form of Dorfin (Dorfin$^{C132S/C135S}$), which lacks E3 activity (Ishigaki et al., 2004), degraded significantly more slowly than did Dorfin^{WT} (Fig. 1A and Table 1). As shown in Fig. 1A, Dorfin^{WT} showed two bands, whereas Dorfin$^{C132S/C135S}$ had a single band. This was also seen in our previous study (Ishigaki et al., 2004) and may represent posttranslational modification.

Construction of Dorfin-CHIP chimeric proteins

It is known that the C-terminus portion of Dorfin can bind to substrates such as mutant SOD1 proteins or Synphilin-1 (Niwa et al., 2002; Ito et al., 2003). We attempted to identify the domain of Dorfin that interacts with substrates. Although there was no obvious known motif in the C-terminus of Dorfin (amino acids 333–838), its first quarter contained rich hydrophobic amino acids (amino acids 333–454) (Fig. 2A). Immunoprecipitation analysis revealed that the hydrophobic region of Dorfin (amino acids 333–454) was able to bind to SOD1^{G85R}, indicating that this hydrophobic region is responsible for recruiting mutant SOD1 in Dorfin protein (Fig. 2B).

To establish more effective and more stable E3 ubiquitin ligase molecules that can recognize and degrade mutant SOD1s, we

Table 1
Serial changes in the amounts of Dorfin^{WT}, Dorfin$^{C132S/C135S}$, and Dorfin-CHIP^{L}

	0 h (%)	1 h (%)	3 h (%)
Dorfin^{WT}	100	43.7±7.0	10.3±4.4
Dorfin$^{C132S/C135S}$	100	73.9±13.8	43.7±1.9
Dorfin-CHIP^{L}	100	89.0±5.7	47.5±5.3

Values are the mean and SD of four independent experiments.

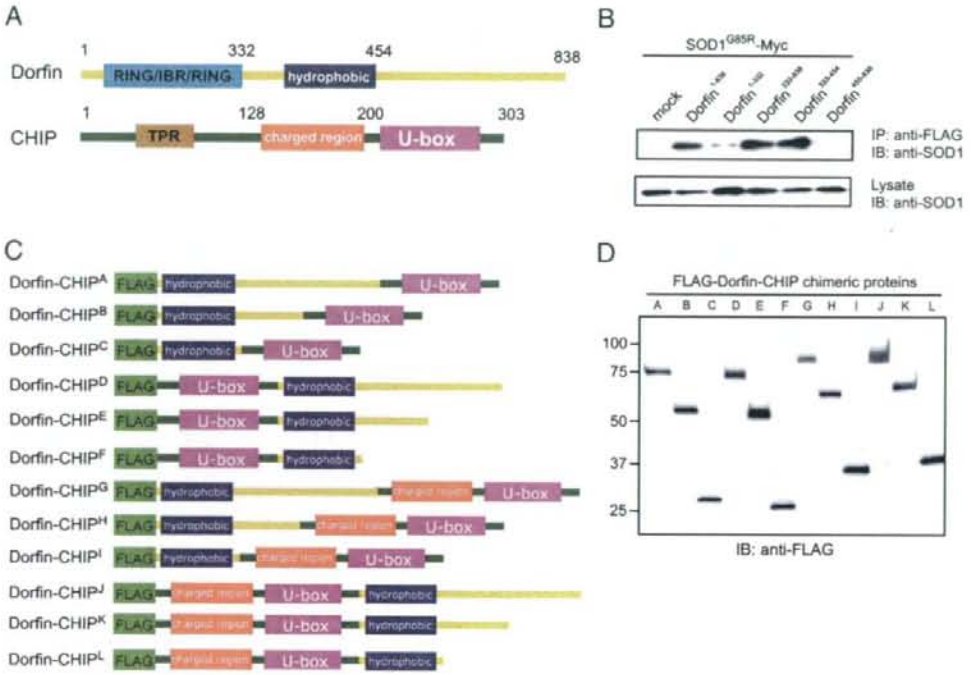

Fig. 2. Construction of Dorfin-CHIP chimeric proteins. (A) Dorfin has a RING/IBR domain in its N-terminus and a substrate-binding portion in the C-terminus. CHIP contains a TPR domain that binds to heat-shock proteins at the N-terminus; its C-terminal U-box domain has strong E3 ubiquitin ligase activity. (B) SOD1^{G85R}-Myc and FLAG-Dorfin derivatives were overexpressed in HEK 293 cells. Cell lysates were immunoprecipitated with anti-myc antibody. Immunoblotting showed that FLAG-Dorfin derivatives containing Dorfin$^{333-454}$ bound to SOD1^{G85R}-Myc, indicating that the hydrophobic region of Dorfin (Dorfin$^{333-454}$) is essential for interaction with mutant SOD1 *in vivo*. (C) Scheme of engineered Dorfin-CHIP chimeric proteins. Three different lengths of C-terminal Dorfin containing the hydrophobic region of Dorfin (Dorfin$^{333-454}$) and the U-box domain of CHIP with or without the charged region were fused. (D) Dorfin-CHIP chimeric proteins were overexpressed in HEK293 cells. Harvested cells were lysed and analyzed by immunoblotting using anti-FLAG antibody.

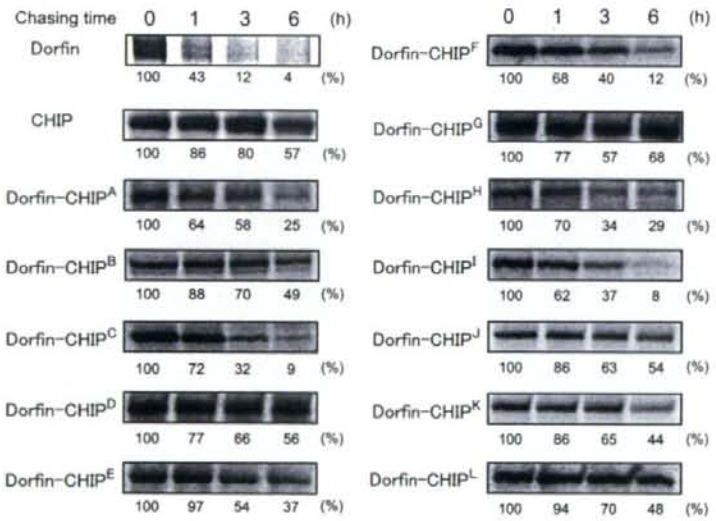

Fig. 3. The stability of Dorfin-CHIP chimeric proteins. Pulse-chase analysis using [^{35}S]-Met/Cys was performed. Dorfin, CHIP, and all the Dorfin-CHIP chimeric proteins were overexpressed in HEK293 cells and labeled with [^{35}S]-Met/Cys. Immunoprecipitation using anti-FLAG antibody and SOD-PAGE analysis revealed the degradation speed of FLAG-Dorfin-CHIP chimeric proteins. The amount of each Dorfin-CHIP chimeric protein was measured by quantifying the band using ImageGauge software.

designed Dorfin-CHIP chimeric proteins containing both the hydrophobic substrate-binding domain of Dorfin and the U-box domain of CHIP, which has strong E3 activity (Fig. 2C). We verified that all of the 12 candidate chimeric proteins were expressed in HEK293 cells (Fig. 2D).

Expression of Dorfin-CHIP chimeric proteins in cells

The half lives of all the Dorfin-CHIP chimeric proteins were more than 1 h. In some of these proteins, such as Dorfin-CHIP$^{D, G, J}$, and ^{L}, moderate amounts of protein still remained at 6 h after labeling, indicating that they were degraded much more slowly than was Dorfin^{WT} (Fig. 3). Repetitive experiments using Dorfin-CHIP^{L} yielded a significant difference between the amount of Dorfin^{WT} and Dorfin-CHIP^{L} at 1 h and 3 h (Table 1).

E3 activity of Dorfin-CHIP chimeric proteins against mutant SOD1

Immunoprecipitation analysis demonstrated that Dorfin and CHIP bound to mutant SOD1^{G85R} in equivalent amounts and that all of the Dorfin-CHIP chimeric proteins interacted with mutant SOD1^{G85R} *in vivo*. Dorfin-CHIP$^{A, D, E, F, J, K}$, and ^{L} bound to the same or greater amounts of SOD1^{G85R} than did Dorfin, whereas Dorfin-CHIP$^{B, C, G, H}$, and ^{I} did not (Fig. 4A, upper panel). None of the Dorfin-CHIP chimeric proteins bound to SOD1^{WT} *in vivo*

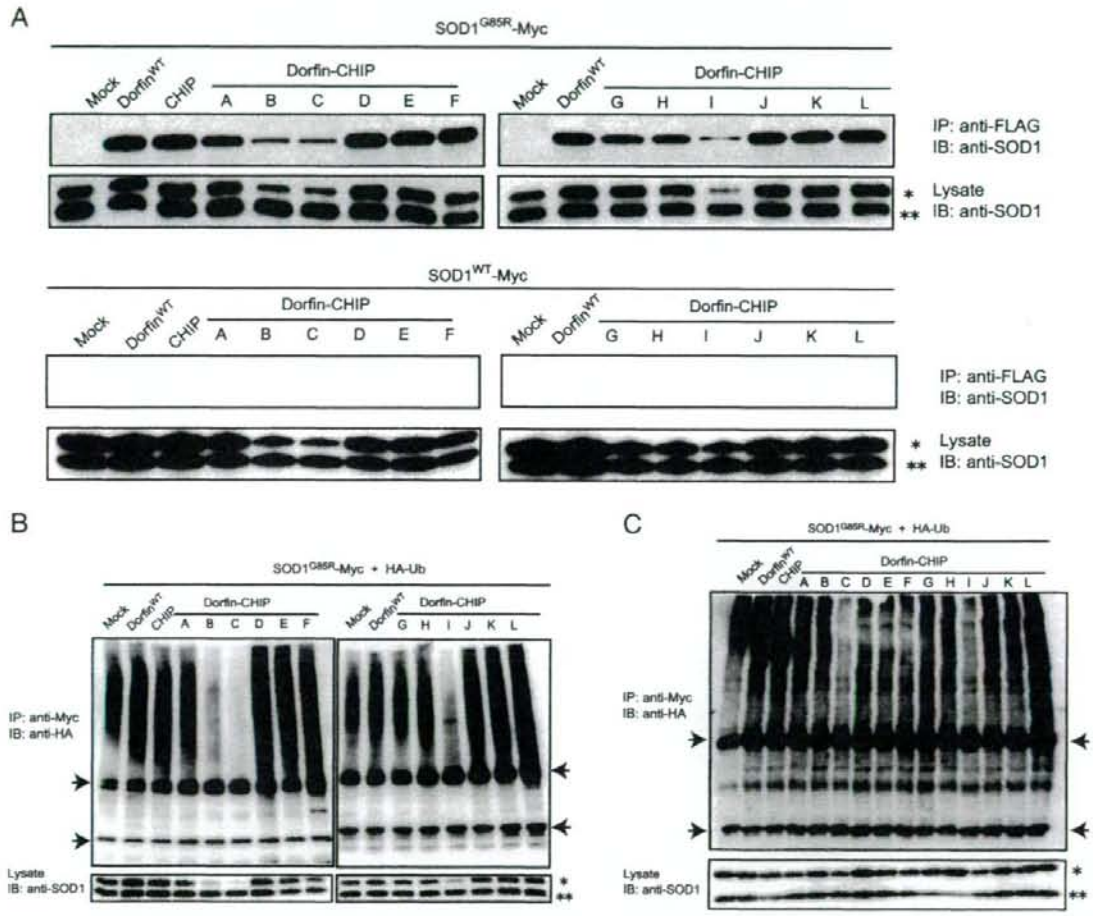

Fig. 4. The E3 activity of Dorfin-CHIP chimeric proteins on mutant SOD1 *in vivo*. (A) *In vivo* binding assay with both wild-type and mutant SOD1s. SOD1^{G85R}- or SOD1^{WT}-Myc and FLAG derivatives of Dorfin-CHIP chimeric proteins were coexpressed in HEK293 cells. Immunoprecipitation was done using anti-Myc antibody. Immunoblotting with anti-FLAG antibody revealed that all the Dorfin-CHIP chimeric proteins bound *in vivo* to SOD1^{G85R}-Myc but not to SOD1^{WT}-Myc. Single and double asterisks indicate overexpressed human SOD1s and mouse endogenous SOD1, respectively. (B) *In vivo* ubiquitylation assay in HEK293 cells. SOD1^{G85R}-Myc, HA-Ub, and FLAG derivatives of Dorfin-CHIP chimeric proteins were coexpressed in HEK293 cells. Immunoblotting with anti-HA antibody demonstrated the ubiquitylation level of SOD1^{G85R}-Myc by FLAG derivatives of Dorfin-CHIP chimeric proteins *in vivo*. Arrows indicate IgG light and heavy chains. Single and double asterisks indicate overexpressed SOD1 and mouse endogenous SOD1, respectively. (C) *In vivo* ubiquitylation assay in N2a cells. SOD1^{G85R}-Myc, HA-Ub, and FLAG derivatives of Dorfin-CHIP chimeric proteins were coexpressed in N2a cells. Arrows indicate IgG light and heavy chains. Single and double asterisks indicate overexpressed human SOD1s and mouse endogenous SOD1, respectively.

(Fig. 4A, lower panel). Some Dorfin-CHIP chimeric proteins, such as Dorfin-CHIP$^{B, C}$, and ^{I}, had lower amounts of both SOD1^{WT} and SOD1^{G85R} in the lysates. We performed quantitative RT-PCR using specific primers for SOD1-Myc, finding that coexpression of Dorfin-CHIP$^{B, C}$ or ^{I} suppressed the mRNA expression of overexpressed SOD1 gene (Supplementary Fig. 1). Considering the possibility that these Dorfin-CHIP chimeric proteins might have unpredicted toxicity for cells by affecting gene transcription via unknown mechanisms, we excluded them from further analysis. Other Dorfin-CHIP proteins did not affect SOD1-Myc gene expression, which validated the comparison among IPs and ubiquitylated mutant SOD1 in Figs. 4A–C.

To assess the effectiveness of the E3 activity of Dorfin-CHIP chimeric proteins, we did an *in-vivo* ubiquitylation analysis by coexpression of SOD1^{G85R}-Myc, HA-Ub, and Dorfin-CHIP chimeric proteins in HEK293 cells. We found that Dorfin and CHIP enhanced the ubiquitylation of SOD1^{G85R} protein and that the ubiquitylation levels of these two E3 ligases were almost equivalent. Moreover, Dorfin-CHIP$^{D, E, F, J, K}$, and ^{L} ubiquitylated SOD1^{G85R} more effectively than did Dorfin or CHIP (Fig. 4B).

Performing the same *in-vivo* ubiquitylation assay using N2a cells, we observed that the levels of ubiquitylation of SOD1^{G85R} by Dorfin and CHIP were equivalent, as they were in HEK293 cells. Among Dorfin-CHIP chimeric proteins, only Dorfin-CHIP^{L}

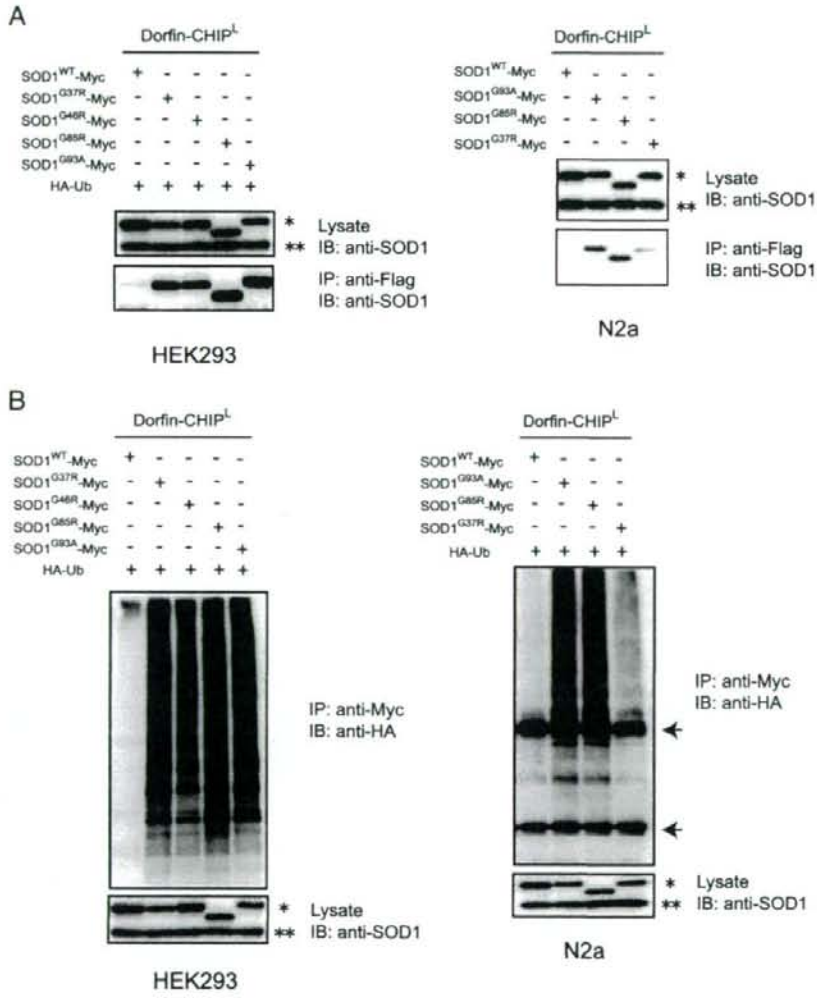

Fig. 5. Dorfin-CHIP^{L} specifically ubiquitylates mutant SOD1s *in vivo*. (A) *In vivo* binding assay with various mutant SOD1s. SOD1^{WT}-Myc, SOD1^{G93A}-Myc, SOD1^{G85R}-Myc, SOD1^{H46R}-Myc or SOD1^{G37R}-Myc, and FLAG-Dorfin-CHIP^{L} were coexpressed in HEK293 (left) and N2a cells (right). Immunoprecipitation was done using anti-Myc antibody. Immunoblotting with anti-FLAG antibody showed that both chimeric proteins specifically bound to mutant SOD1s *in vivo*. Single and double asterisks indicate overexpressed SOD1 and mouse endogenous SOD1, respectively. (B) *In vivo* ubiquitylation assay. SOD1^{WT}-Myc, SOD1^{G93A}-Myc, SOD1^{G85R}-Myc, SOD1^{H46R}-Myc or SOD1^{G37R}-Myc, as well as FLAG-Dorfin-CHIP^{L} and HA-Ub, was coexpressed in HEK293 (left) and N2a cells (right). Immunoblotting with anti-HA antibody showed the specific ubiquitylation of mutant SOD1-Myc by FLAG-Dorfin-CHIP^{L} *in vivo*. Arrows indicate IgG light and heavy chains. Single and double asterisks indicate overexpressed human SOD1s and mouse endogenous SOD1, respectively.

ubiquitylated SOD1^{G85R} more effectively than did Dorfin or CHIP, while Dorfin-CHIP$^{D, E, F, J}$, and ^{K} did not (Fig. 4C). Thus, Dorfin-CHIP^{L} was the most potent candidate of the chimeric proteins.

Ubiquitylation of mutant SOD1 by Dorfin-CHIP^{L}

Dorfin specifically ubiquitylated mutant SOD1 proteins, but not SOD1^{WT} protein (Niwa et al., 2002; Ishigaki et al., 2004). Similarly, Dorfin-CHIP^{L} interacted with SOD1^{G93A}, SOD1^{G85R}, SOD1^{H46R}, and SOD1^{G37R}, but not SOD1^{WT}, in HEK293 cells. This was confirmed in N2a cells (Fig. 5A). In both HEK293 and N2a cells, Dorfin-CHIP^{L} also ubiquitylated mutant SOD1 proteins but not SOD1^{WT} (Fig. 5B).

Degradation of mutant SOD1 by Dorfin-CHIP chimeric proteins

To assess the degradation activity of Dorfin-CHIP^{L} against mutant SOD1s, we performed the pulse-chase analysis on N2a

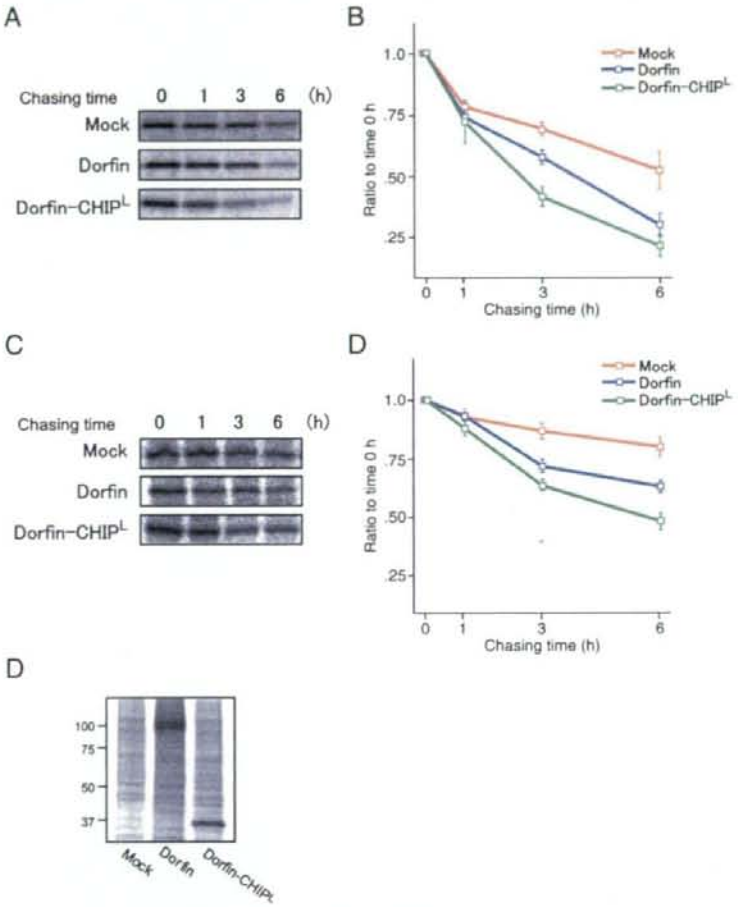

Fig. 6. Degradation of mutant SOD1 proteins with Dorfin-CHIP^{L}. (A) Pulse-chase analysis of SOD1^{G85R} with Dorfin-CHIP^{L}. N2a cells were coexpressed with SOD1^{G85R}-Myc and Mock, Dorfin, and Dorfin-CHIP^{L}. Pulse-chase experiments using [^{35}S]-Met/Cys were done. Immunoprecipitation using anti-Myc antibody and SOD-PAGE analysis revealed the degradation speed of SOD1^{G85R}-Myc. (B) Serial changes in the amount of SOD1^{G85R} coexpressed with Mock, Dorfin, or Dorfin-CHIP^{L}. Four independent experiments were performed and the amounts of SOD1^{G85R} were plotted. There were significant differences between Mock and Dorfin ($p<0.005$), Mock and Dorfin-CHIP^{L} ($p<0.005$), and Dorfin and Dorfin-CHIP^{L} ($p<0.05$) at 3 h, as well as between Mock and Dorfin ($p<0.05$), and Mock and Dorfin-CHIP^{L} ($p<0.05$) at 6 h after labeling. Values are the means ± SE, $n=4$. Statistical analysis was done by one-way ANOVA. (C) Pulse-chase analysis of SOD1^{G93A} with Dorfin-CHIP^{L}. N2a cells were coexpressed with SOD1^{G93A}-Myc and Mock, Dorfin, and Dorfin-CHIP^{L} as in panel A. (D) Serial changes in the amount of SOD1^{G93A} coexpressed with Mock, Dorfin, or Dorfin-CHIP^{L}. Four independent experiments were performed and the amounts of SOD1^{G93A} were plotted. There were significant differences between Mock and Dorfin ($p<0.05$) and Mock and Dorfin-CHIP^{L} ($p<0.01$) at 3 h, as well as between Mock and Dorfin ($p<0.05$), Mock and Dorfin-CHIP^{L} ($p<0.01$), and Dorfin and Dorfin-CHIP^{L} ($p<0.05$) at 6 h after labeling. Values are the means ± SE, $n=4$. Statistics were done by one-way ANOVA. (E) The equivalent protein expression levels of Dorfin and Dorfin-CHIP^{L}. Half of the volume of samples used in the pulse-chase analysis of panel C at 0 h was used for immunoprecipitation using anti-Flag M2 antibody. The following SOD-PAGE analysis revealed the amounts of Dorfin and Dorfin-CHIP^{L} in the experiment shown in panel C.

cells, using [^{35}S] labeled Met/Cys. The protein levels of SOD1^{G85R} and SOD1^{G93A} declined more rapidly with Dorfin coexpression. Dorfin-CHIP^{L} remarkably declined in both SOD1^{G85R} and SOD1^{G93A} (Figs. 6A, C). Dorfin and Dorfin-CHIP^{L} had similar expression levels at 0 h of this experiment (Fig. 6E). As compared to Mock, Dorfin showed significant declines of both SOD1^{G85R} at 3 h ($p<0.001$) and 6 h ($p<0.05$) after labeling, as shown in a previous study (Niwa et al., 2002). Dorfin-CHIP^{L} also significantly accelerated the decline of SOD1^{G85R} at 3 h ($p<0.001$) and 6 h ($p<0.05$) after labeling again as compared to Mock. At 3 h after labeling, a significant difference between Dorfin-CHIP^{L} and Dorfin was present with respect to SOD1^{G85R} degradation ($p<0.05$). As compared to Dorfin, Dorfin-CHIP^{L} also tended toward accelerated SOD1^{G85R} degradation at 6 h after labeling (Fig. 6B). Similarly, Dorfin showed significant declines of SOD1^{G93A} at 3 h ($p<0.05$) and 6 h ($p<0.05$) after labeling, and Dorfin-CHIP^{L} significantly accelerated the declines of SOD1^{G93A} at 3 h ($p<0.01$) and 6 h ($p<0.01$) after labeling as compared to Mock. A significant difference between Dorfin-CHIP^{L} and Dorfin was present at 6 h in SOD1^{G93A} degradation ($p<0.05$) (Fig. 6D).

Attenuation of the toxicity of mutant SOD1 and decrease in the formation of visible aggregations of mutant SOD1 in cultured neuronal culture cells

The ability of Dorfin-CHIP chimeric proteins to attenuate mutant SOD1-related toxicity was analyzed by MTS assay using N2a cells. The expression of SOD1^{G85R}, as compared to that of SOD1^{WT}, decreased the viability of cells. Overexpression of Dorfin reversed the toxic effect of SOD1^{G85R}, whereas overexpression of CHIP did not. Dorfin-CHIP^{L} had a significantly greater rescue effect on SOD1^{G85R}-related cell toxicity than did Dorfin (Fig. 7A). We also measured the cell viability of N2a cells overexpressing Mock, Dorfin, and Dorfin-CHIP^{L} with various amounts of constructs, and found no difference in toxicity among them (Supplementary Fig. 2).

A structure that Johnston et al. (1998) called aggresome is formed when the capacity of a cell to degrade misfolded proteins is exceeded. The accumulation of mutant SOD1 induces visible macroaggregation, which is considered to be 'aggresome' in N2a cells. We examined the subcellular localizations of Dorfin, CHIP, and Dorfin-CHIP^{L} by immunostaining N2a cells expressing SOD1^{G85R}-GFP. Dorfin was localized in aggresomes with substrate proteins, as in our previous studies. Dorfin-CHIP^{L} was also seen in aggresomes, whereas the staining of CHIP was diffusely observed in the cytosol (Fig. 7B). We counted these visible aggregations with or without MG132 treatment. Dorfin decreased the number of aggregation-containing cells, as has been reported (Niwa et al., 2002), but Dorfin-CHIP^{L} did so more effectively. These effects were inhibited by the treatment of MG132 (Fig. 7C).

Discussion

E3 proteins can specifically recognize and degrade accumulating aberrant proteins, which are deeply involved in the pathogenesis of neurodegenerative disorders, including ALS (Alves-Rodrigues et al., 1998; Sherman and Goldberg, 2001; Ciechanover and Brundin, 2003). For this reason, E3 proteins are candidate molecules for use in developing therapeutic technology for neurodegenerative diseases. Dorfin is the first E3 molecule that has been found specifically to ubiquitylate mutant SOD1 proteins as well as to attenuate mutant SOD-associated toxicity in cultured neuronal cells (Niwa et al., 2002).

NEDL1, a HECT type E3 ligase, has also been reported to be a mutant SOD1-specific E3 ligase and to interact with TRAPδ and dvl1 (Miyazaki et al., 2004). It has also been reported that ubiquitylation of mutant SOD1-associated complex was enhanced by CHIP and Hsp70 *in vivo* (Urushitani et al., 2004). CHIP ubiquitylated Hsp70-holding SOD1 complexes and degraded mutant SOD1, but did not directly interact with mutant SOD1 (Urushitani et al., 2004). Among these E3 molecules, Dorfin seems to be the most potentially beneficial E3 protein for use in ALS therapy since it is the only one that has been demonstrated to reverse mutant SOD1-associated toxicity (Niwa et al., 2002). Furthermore, Dorfin has been localized in various ubiquitin-positive inclusions such as Lewy bodies (LB) in PD, as well as LB-like inclusions in sporadic ALS and glial cell bodies in multiple-system atrophy. These findings indicate that Dorfin may be involved in the pathogenesis of a broad spectrum of neurodegenerative disorders other than familial ALS (Hishikawa et al., 2003; Ito et al., 2003; Ishigaki et al., 2004).

The half-life of Dorfin^{WT} is, however, less than 1 h (Fig. 1, Table 1). The amount of Dorfin is increased in the presence of MG132, a proteasome inhibitor, indicating that Dorfin is immediately degraded in the UPS. Since the nonfunctional RING mutant form of Dorfin, Dorfin$^{C132S/C135S}$, degraded more slowly than did Dorfin^{WT}, Dorfin seemed to be degraded by auto-ubiquitylation. The degradation of Dorfin$^{C132S/C135S}$ is also inhibited by MG132, suggesting that it is degraded by endogenous Dorfin or other E3s. This immediate degradation of Dorfin is a serious problem for its therapeutic application against neurodegenerative diseases.

Several reports have shown that engineered chimera E3s are able to degrade certain substrates with high efficiency. Protac, a chimeric protein-targeting molecule, was designed to target methionine aminopeptidase-2 to Skp1-Cullin-F box complex (SCF) ubiquitin ligase complex for ubiquitylation and degradation (Sakamoto et al.,

Fig. 7. Dorfin-CHIP chimeric proteins can attenuate toxicity induced by mutant SOD1 and decrease the formation of visible aggregation of mutant SOD1 in N2a cells. (A) N2a cells were grown in 96 collagen-coated wells (5000 cells per well) and transfected with 0.15 μg of SOD1^{WT} and 0.05 μg of Mock or 0.15 μg of SOD1^{G85R} and 0.05 μg of Mock, Dorfin, CHIP, or Dorfin-CHIP^{L}. After the medium was changed, MTS assays were done at 48 h of incubation. Viability was measured as the level of absorbance (490 nm). Values are the means±SE, $n=6$. Statistics were carried out by one-way ANOVA. There were significant differences between SOD1^{G85R}-expressing cells coexpressed with Mock and SOD1^{G85R}-expressing cells coexpressed with Dorfin ($p<0.001$), as well as between SOD1^{G85R}-expressing cells coexpressed with Dorfin and SOD1^{G85R}-expressing cells coexpressed with Dorfin-CHIP^{L} ($p<0.001$). (B) N2a cells were transiently expressed with SOD1^{G85R}-GFP and Mock, Dorfin, CHIP, or Dorfin-CHIP^{L}. Immunostaining with anti-FLAG antibody revealed that Dorfin, CHIP, and Dorfin-CHIP^{L} were localized with SOD1^{G85R}-GFP in macroaggresomes (arrows). Scale bar=20 μm (C) The visible macroaggregations in N2a cells expressing both SOD1^{G85R}-GFP and Mock, Dorfin, CHIP, or Dorfin-CHIP^{L} with or without MG132 treatment were counted and the ratio of cells with aggregations to those with GFP signals was calculated. Values are the means±SE, $n=4$. Statistics were done by one-way ANOVA. *$p<0.01$ denotes a significant difference between cells with Mock and Dorfin or Dorfin-CHIP^{L}. **$p<0.05$ denotes a significant difference between cells with Dorfin and Dorfin-CHIP^{L}.

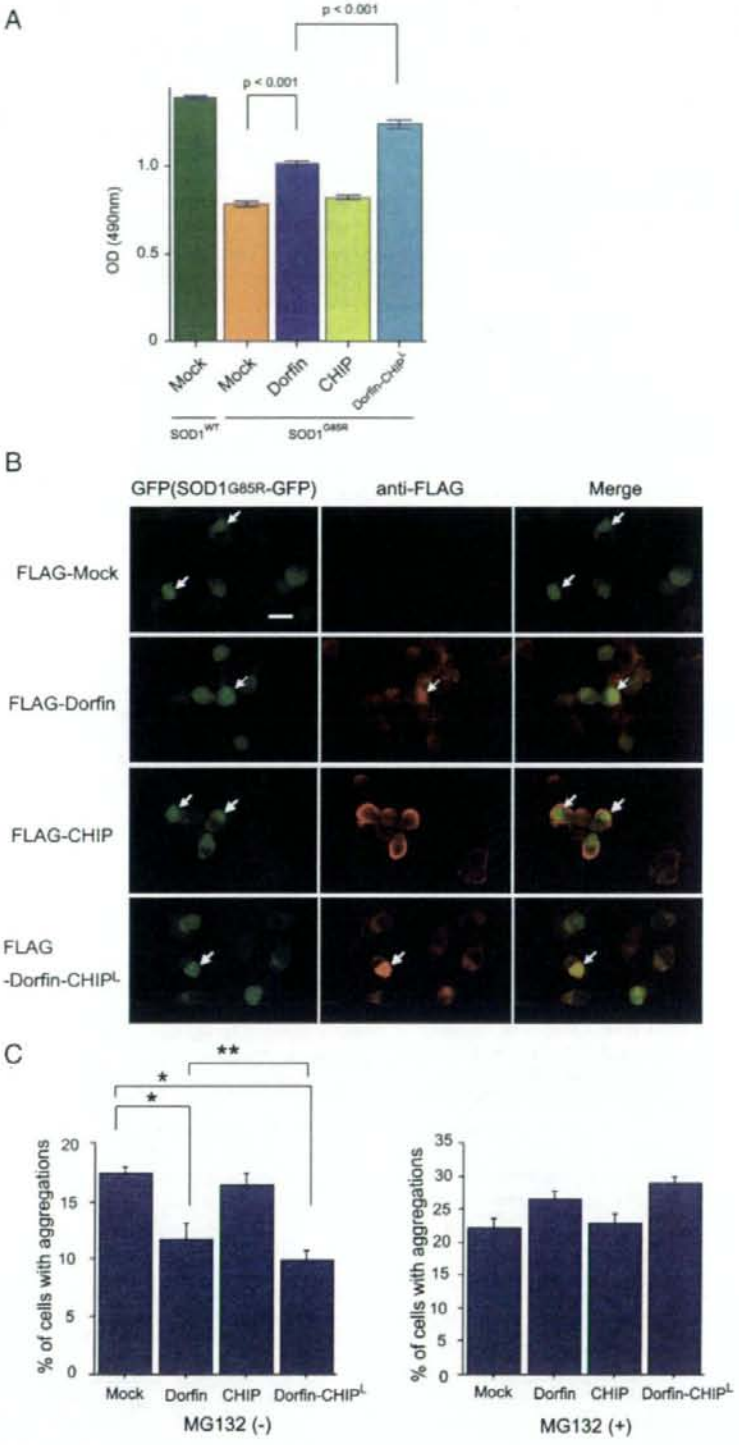
A
p < 0.001
p < 0.001
OD (490nm)
1.0
0.5
0
Mock
Mock
Dorfin
CHIP
Dorfin-CHIP^L
SOD1^WT
SOD1^G85R
B
GFP(SOD1G85R-GFP)
anti-FLAG
Merge
FLAG-Mock
FLAG-Dorfin
FLAG-CHIP
FLAG
-Dorfin-CHIP^L
C
**
*
*
% of cells with aggregations
20
15
10
5
0
Mock
Dorfin
CHIP
Dorfin-CHIP^L
MG132 (-)
% of cells with aggregations
35
30
25
20
15
10
5
0
Mock
Dorfin
CHIP
Dorfin-CHIP^L
MG132 (+)

2001, 2003). Oyake et al. (2002) developed double RING ubiquitin ligases containing the RING finger domains of both BRCA and BARD1 linked to a substrate recognition site PCNA. Recently, Hatakeyama et al. developed a fusion protein composed of Max, which forms a heterodimer with c-Myc, and the U-box of CHIP. This fusion protein physically interacted with c-Myc and promoted the ubiquitylation of c-Myc. It also reduced the stability of c-Myc, resulting in the suppression of transcriptional activity dependent on c-Myc and the inhibition of tumorogenesis (Hatakeyama et al., 2005). This indicated that the U-box portion of CHIP is able to add an effective E3 function to a U-box-containing client protein.

We postulated that engineered forms of Dorfin could be stable and still function as specific E3s for mutant SOD1s. Dorfin has a RING/IBR domain in the N-terminal portion (amino acids 1-332), but has no obvious motif in the rest of the C-terminus (amino acids 333–838). In this study, we have demonstrated that the hydrophobic domain of Dorfin (amino acids 333–454) is both necessary and sufficient for substrate recruiting (Fig. 2B). In our engineered proteins, the RING/IBR motif of N-terminal Dorfin was replaced by the UPR domain of CHIP, which had strong E3 activity (Murata et al., 2001). Some of the engineered Dorfin-chimeric proteins, such as Dorfin-CHIP$^{D, G, J}$, and ^{L}, were degraded *in vivo* far more slowly than was wild-type Dorfin, indicating that they were capable of being stably presented *in vivo* (Fig. 3). However, Dorfin-CHIP^{G} failed to show strong ubiquitylation activity against SOD1^{G85R} in HEK293 cells. Since Dorfin-CHIP$^{D, J}$, and ^{L} were able to bind to SOD1^{G85R} more strongly than did Dorfin-CHIP^{G}, the binding activity was more important for the E3 activity than for the protein stability.

We next showed that although all of the Dorfin-CHIP chimeric proteins bound to mutant SOD1 *in vivo*, some of them, such as Dorfin-CHIP$^{B, C}$, and ^{I}, bound less than others (Fig. 4A). In HEK293 cells, Dorfin-CHIP$^{D, E, F, J, K}$, and ^{L} ubiquitylated SOD1^{G85R} more effectively than did Dorfin or CHIP; however, in N2a cells only Dorfin-CHIP^{L} had more effective E3 activity than did Dorfin or CHIP. This discrepancy may be due to differences between HEK 293 and N2a cells which could provide slight different environment for the E3 machinery. Therefore, Dorfin-CHIP^{L} was the most potent of the candidate chimeric proteins in degrading mutant SOD1 in the UPS in neuronal cells. We also showed that Dorfin-CHIP^{L} could specifically bind to and ubiquitylate mutant SOD1s but not SOD1^{WT} *in vivo*, as Dorfin had done (Niwa et al., 2002; Ishigaki et al., 2004) (Fig. 5). This observation confirmed that the hydrophobic domain of Dorfin (amino acids 333–454) is responsible for mutant SOD1 recruiting.

Pulse-chase analysis using N2a cells showed that Dorfin-CHIP^{L} degraded SOD1^{G85R} and SOD1^{G93A} more effectively than did Dorfin (Fig. 6). This is compatible with the finding that Dorfin-CHIP^{L} had a greater effect than Dorfin did on the ubiquitylation against mutant SOD1. The cycloheximide assay verified that the degradation ability of Dorfin-CHIP^{L} against SOD1^{G85R} was stronger than that of Dorfin or CHIP in HEK293 cells (data not shown).

Dorfin-CHIP^{L} also reversed SOD1^{G85R}-associated toxicity in N2a cells more effectively than did Dorfin (Fig. 7). This therapeutic effect of Dorfin-CHIP^{L} was expected from its strong E3 activity and degradation ability against SOD1^{G85R}. Visible protein aggregations have been considered to be hallmarks of neurodegeneration. Increased understanding of the pathway involved in protein aggregation may demonstrate that visible macroaggregates represent the end-stage of a molecular cascade of steps rather than a direct toxic insult (Ross and Poirier, 2004). Two facts that Dorfin-CHIP^{L} decreased aggregation formation of SOD1^{G85R} and that this effect was inhibited by a proteasome inhibitor should reflect the ability of Dorfin-CHIP^{L} to degrade mutant SOD1 in the UPS of cells.

Based on our present observations, Dorfin-CHIP^{L}, an engineered chimeric molecule with the hydrophobic substrate-binding domain of Dorfin and the U-box domain of CHIP, had stronger E3 activity against mutant SOD1 than did Dorfin or CHIP. Indeed, it not only degraded mutant SOD1 more effectively than did Dorfin or CHIP but, as compared to Dorfin, produced marked attenuation of mutant SOD1-associated toxicity in N2a cells. This protective effect of Dorfin-CHIP^{L} against mutant SOD1 has potential applications to gene therapy for mutant SOD1 transgenic mice because this protein has a long enough life to allow the constant removal of mutant SOD1 from neurons. Since Dorfin was originally identified as a sporadic ALS-associated molecule (Ishigaki et al., 2002b) and is located in the ubiquitin-positive inclusions of various neurodegenerative diseases (Hishikawa et al., 2003), this molecule is an appropriate candidate for future use in gene therapy not only for familial ALS, but also for sporadic ALS and other neurodegenerative disorders.

So far, most reports on engineered chimera E3s have targeted cancer-promoting proteins. Dorfin-CHIP chimeric proteins are the first chimera E3s to be intended for the treatment of neurodegenerative diseases. Since the accumulation of ubiquitylated proteins in neurons is a pathological hallmark of various neurodegenerative diseases, development of chimera E3s like Dorfin-CHIP^{L}, which can remove unnecessary proteins, is a new therapeutic concept. Further analysis, including transgenic overexpression and vector delivery of Dorfin-CHIP chimeric proteins using ALS animal models will increase our understanding of the potential utility of Dorfin-CHIP chimeric proteins as therapeutic tools.

Acknowledgments

We gratefully thank Dr. Shigetsugu Hatakeyama at Hokkaido University for his advice about the construction of Dorfin-CHIP chimeric proteins. This work was supported by the Nakabayashi Trust for ALS Research; a grant for Center of Excellence (COE) from the Ministry of Education, Culture, Sports, Science and Technology of Japan; and grants from the Ministry of Health, Welfare and Labor of Japan.

Appendix A. Supplementary data

Supplementary data associated with this article can be found, in the online version, at doi:10.1016/j.nbd.2006.09.017.

References

Alves-Rodrigues, A., Gregori, L., Figueiredo-Pereira, M.E., 1998. Ubiquitin, cellular inclusions and their role in neurodegeneration. Trends Neurosci. 21, 516–520.

Bercovich, B., Stancovski, I., Mayer, A., Blumenfeld, N., Laszlo, A., Schwartz, A.L., Ciechanover, A., 1997. Ubiquitin-dependent degradation of certain protein substrates in vitro requires the molecular chaperone Hsc70. J. Biol. Chem. 272, 9002–9010.

Ciechanover, A., Brundin, P., 2003. The ubiquitin proteasome system in

neurodegenerative diseases: sometimes the chicken, sometimes the egg. Neuron 40, 427–446.

Cudkowicz, M.E., McKenna-Yasek, D., Sapp, P.E., Chin, W., Geller, B., Hayden, D.L., Schoenfeld, D.A., Hosler, B.A., Horvitz, H.R., Brown, R.H., 1997. Epidemiology of mutations in superoxide dismutase in amyotrophic lateral sclerosis. Ann. Neurol. 41, 210–221.

Glickman, M.H., Ciechanover, A., 2002. The ubiquitin–proteasome proteolytic pathway: destruction for the sake of construction. Physiol. Rev. 82, 373–428.

Hatakeyama, S., Matsumoto, M., Kamura, T., Murayama, M., Chui, D.H., Planel, E., Takahashi, R., Nakayama, K.I., Takashima, A., 2004. U-box protein carboxyl terminus of Hsc70-interacting protein (CHIP) mediates poly-ubiquitylation preferentially on four-repeat Tau and is involved in neurodegeneration of tauopathy. J. Neurochem. 91, 299–307.

Hatakeyama, S., Watanabe, M., Fujii, Y., Nakayama, K.I., 2005. Targeted destruction of c-Myc by an engineered ubiquitin ligase suppresses cell transformation and tumor formation. Cancer Res. 65, 7874–7879.

Hishikawa, N., Niwa, J., Doyu, M., Ito, T., Ishigaki, S., Hashizume, Y., Sobue, G., 2003. Dorfin localizes to the ubiquitylated inclusions in Parkinson's disease, dementia with Lewy bodies, multiple system atrophy, and amyotrophic lateral sclerosis. Am. J. Pathol. 163, 609–619.

Ishigaki, S., Liang, Y., Yamamoto, M., Niwa, J., Ando, Y., Yoshihara, T., Takeuchi, H., Doyu, M., Sobue, G., 2002a. X-Linked inhibitor of apoptosis protein is involved in mutant SOD1-mediated neuronal degeneration. J. Neurochem. 82, 576–584.

Ishigaki, S., Niwa, J., Ando, Y., Yoshihara, T., Sawada, K., Doyu, M., Yamamoto, M., Kato, K., Yotsumoto, Y., Sobue, G., 2002b. Differentially expressed genes in sporadic amyotrophic lateral sclerosis spinal cords—Screening by molecular indexing and subsequent cDNA microarray analysis. FEBS Lett. 531, 354–358.

Ishigaki, S., Hishikawa, N., Niwa, J., Iemura, S., Natsume, T., Hori, S., Kakizuka, A., Tanaka, K., Sobue, G., 2004. Physical and functional interaction between Dorfin and Valosin-containing protein that are colocalized in ubiquitylated inclusions in neurodegenerative disorders. J. Biol. Chem. 279, 51376–51385.

Ito, T., Niwa, J., Hishikawa, N., Ishigaki, S., Doyu, M., Sobue, G., 2003. Dorfin localizes to Lewy bodies and ubiquitylates synphilin-1. J. Biol. Chem. 278, 29106–29114.

Johnston, J.A., Ward, C.L., Kopito, R.R., 1998. Aggresomes: a cellular response to misfolded proteins. J. Cell Biol. 143, 1883–1898.

Julien, J.P., 2001. Amyotrophic lateral sclerosis. unfolding the toxicity of the misfolded. Cell 104, 581–591.

Jungmann, J., Reins, H.A., Schobert, C., Jentsch, S., 1993. Resistance to cadmium mediated by ubiquitin-dependent proteolysis. Nature 361, 369–371.

Lee, D.H., Sherman, M.Y., Goldberg, A.L., 1996. Involvement of the molecular chaperone Ydj1 in the ubiquitin-dependent degradation of short-lived and abnormal proteins in *Saccharomyces cerevisiae*. Mol. Cell. Biol. 16, 4773–4781.

Meacham, G.C., Patterson, C., Zhang, W., Younger, J.M., Cyr, D.M., 2001. The Hsc70 co-chaperone CHIP targets immature CFTR for proteasomal degradation. Nat. Cell Biol. 3, 100–105.

Miyazaki, K., Fujita, T., Ozaki, T., Kato, C., Kurose, Y., Sakamoto, M., Kato, S., Goto, T., Itoyama, Y., Aoki, M., Nakagawara, A., 2004. NEDL1, a novel ubiquitin–protein isopeptide ligase for dishevelled-1, targets mutant superoxide dismutase-1. J. Biol. Chem. 279, 11327–11335.

Murata, S., Minami, Y., Minami, M., Chiba, T., Tanaka, K., 2001. CHIP is a chaperone-dependent E3 ligase that ubiquitylates unfolded protein. EMBO Rep. 2, 1133–1138.

Murata, S., Chiba, T., Tanaka, K., 2003. CHIP: a quality-control E3 ligase collaborating with molecular chaperones. Int. J. Biochem. Cell Biol. 35, 572–578.

Niwa, J., Ishigaki, S., Doyu, M., Suzuki, T., Tanaka, K., Sobue, G., 2001. A novel centrosomal ring-finger protein, dorfin, mediates ubiquitin ligase activity. Biochem. Biophys. Res. Commun. 281, 706–713.

Niwa, J., Ishigaki, S., Hishikawa, N., Yamamoto, M., Doyu, M., Murata, S., Tanaka, K., Taniguchi, N., Sobue, G., 2002. Dorfin ubiquitylates mutant SOD1 and prevents mutant SOD1-mediated neurotoxicity. J. Biol. Chem. 277, 36793–36798.

Oyake, D., Nishikawa, H., Kozuka, I., Fukuda, M., Ohta, T., 2002. Targeted substrate degradation by an engineered double RING ubiquitin ligase. Biochem. Biophys. Res. Commun. 295, 370–375.

Rosen, D.R., Siddique, T., Patterson, D., Figlewicz, D.A., Sapp, P., Hentati, A., Donaldson, D., Goto, J., O'Regan, J.P., Deng, H.X., et al., 1993. Mutations in Cu/Zn superoxide dismutase gene are associated with familial amyotrophic lateral sclerosis. Nature 362, 59–62.

Ross, C.A., Poirier, M.A., 2004. Protein aggregation and neurodegenerative disease. Nat. Med. 10, S10–S17 (Suppl.).

Rowland, L.P., Shneider, N.A., 2001. Amyotrophic lateral sclerosis. N. Engl. J. Med. 344, 1688–1700.

Sakamoto, K.M., Kim, K.B., Kumagai, A., Mercurio, F., Crews, C.M., Deshaies, R.J., 2001. Protacs: chimeric molecules that target proteins to the Skp1-Cullin-F box complex for ubiquitination and degradation. Proc. Natl. Acad. Sci. U. S. A. 98, 8554–8559.

Sakamoto, K.M., Kim, K.B., Verma, R., Ransick, A., Stein, B., Crews, C.M., Deshaies, R.J., 2003. Development of Protacs to target cancer-promoting proteins for ubiquitination and degradation. Mol. Cell Proteomics 2, 1350–1358.

Scheffner, M., Nuber, U., Huibregtse, J.M., 1995. Protein ubiquitination involving an E1–E2–E3 enzyme ubiquitin thioester cascade. Nature 373, 81–83.

Sherman, M.Y., Goldberg, A.L., 2001. Cellular defenses against unfolded proteins: a cell biologist thinks about neurodegenerative diseases. Neuron 29, 15–32.

Shimura, H., Schwartz, D., Gygi, S.P., Kosik, K.S., 2004. CHIP–Hsc70 complex ubiquitinates phosphorylated tau and enhances cell survival. J. Biol. Chem. 279, 4869–4876.

Tanaka, K., Suzuki, T., Hattori, N., Mizuno, Y., 2004. Ubiquitin, proteasome and parkin. Biochim. Biophys. Acta 1695, 235–247.

Urushitani, M., Kurisu, J., Tateno, M., Hatakeyama, S., Nakayama, K., Kato, S., Takahashi, R., 2004. CHIP promotes proteasomal degradation of familial ALS-linked mutant SOD1 by ubiquitinating Hsp/Hsc70. J. Neurochem. 90, 231–244.

Yoshida, Y., Tokunaga, F., Chiba, T., Iwai, K., Tanaka, K., Tai, T., 2003. Fbs2 is a new member of the E3 ubiquitin ligase family that recognizes sugar chains. J. Biol. Chem. 278, 43877–43884.

THE JOURNAL OF BIOLOGICAL CHEMISTRY VOL. 282, NO. 38, pp. 28087–28095, September 21, 2007

Disulfide Bond Mediates Aggregation, Toxicity, and Ubiquitylation of Familial Amyotrophic Lateral Sclerosis-linked Mutant SOD1*[S]

Received for publication, May 31, 2007, and in revised form, July 13, 2007 Published, JBC Papers in Press, July 31, 2007, DOI 10.1074/jbc.M704465200

Jun-ichi Niwa[‡§], Shin-ichi Yamada[‡], Shinsuke Ishigaki[‡], Jun Sone[‡], Miho Takahashi[‡], Masahisa Katsuno[‡], Fumiaki Tanaka[‡], Manabu Doyu[‡§], and Gen Sobue[‡1]

From the [‡]Department of Neurology, Nagoya University Graduate School of Medicine, 65 Tsurumai-cho, Showa-ku, Nagoya 466-8500 and the [§]Stroke Center, Aichi Medical University, Aichi 480-1195, Japan

Mutations in the Cu/Zn-superoxide dismutase (*SOD1*) gene cause familial amyotrophic lateral sclerosis (ALS) through the gain of a toxic function; however, the nature of this toxic function remains largely unknown. Ubiquitylated aggregates of mutant SOD1 proteins in affected brain lesions are pathological hallmarks of the disease and are suggested to be involved in several proposed mechanisms of motor neuron death. Recent studies suggest that mutant SOD1 readily forms an incorrect disulfide bond upon mild oxidative stress *in vitro*, and the insoluble SOD1 aggregates in spinal cord of ALS model mice contain multimers cross-linked via intermolecular disulfide bonds. Here we show that a non-physiological intermolecular disulfide bond between cysteines at positions 6 and 111 of mutant SOD1 is important for high molecular weight aggregate formation, ubiquitylation, and neurotoxicity, all of which were dramatically reduced when the pertinent cysteines were replaced in mutant SOD1 expressed in Neuro-2a cells. Dorfin is a ubiquityl ligase that specifically binds familial ALS-linked mutant SOD1 and ubiquitylates it, thereby promoting its degradation. We found that Dorfin ubiquitylated mutant SOD1 by recognizing the Cys^{6}- and Cys^{111}-disulfide cross-linked form and targeted it for proteasomal degradation.

Cu/Zn superoxide dismutase (SOD1),[2] a major intracellular antioxidant enzyme, metabolizes superoxide radicals to molecular oxygen and hydrogen peroxide (1, 2). Because mutations in *SOD1* linked to familial amyotrophic lateral sclerosis (ALS) were first identified (3), more than 100 mutations at over 70 residues in the 153-amino acid SOD1 protein have been reported (4). Most mutations are missense mutations, with a few causing early termination or frame shifts near the carboxyl terminus of the protein. *SOD1* mutations account for ~20% of familial ALS, which is characterized by selective degeneration of motor neurons. SOD1 is primarily a cytosolic protein (5), and the active enzyme is a homodimer of two subunits (6). Each subunit contains four cysteine (Cys) residues at positions 6, 57, 111, and 146. An intramolecular disulfide bond between Cys^{57} and Cys^{146} of each subunit facilitates its correct folding and stabilizes the active homodimeric structure (7, 8), but it is not known how the disulfide is formed in the reducing environment of the cytosol. Although the endoplasmic reticulum is the specialized site for oxidative folding (9), there is no SOD1 localization to the endoplasmic reticulum (10). Most familial ALS-linked mutations render SOD1 more susceptible to intramolecular disulfide bond reduction (11) and accelerate the rate of protein turnover (12, 13). Recent lines of evidence implicate the disulfide-reduced monomer as the common aggregation-prone, neurotoxic intermediate of mutant SOD1 proteins (8, 11, 14–16), and a significant fraction of the insoluble SOD1 aggregates in the spinal cord of mutant SOD1 transgenic mice contains high molecular weight species cross-linked via intermolecular disulfide bonds (17). Hence, modulation of disulfide bond formation may be important in mutant SOD1-linked motor neuron-selective neurotoxicity.

ALS-linked mutant SOD1 proteins are turned over more rapidly than wild-type SOD1, and proteasome inhibitors increase the amount of mutant SOD1 (18, 19). To date, two distinct ubiquityl ligases, Dorfin and NEDL1, have been reported to ubiquitylate mutant SOD1 (20, 21). Dorfin is a RING-finger/IBR (in-between ring-finger) domain-containing ubiquityl ligase, which we previously identified from human spinal cord (22), and belongs to the RBR (RING-Between rings-RING) family of proteins (23). Dorfin physically binds and ubiquitylates various familial ALS-linked SOD1 mutants and subsequently targets them for proteasomal degradation, but it has no effect on the stability of wild-type SOD1 (20). Overexpression of Dorfin protects neuronal cells against the toxic effects of mutant SOD1 and reduces the number of aggregates composed of mutant SOD1 (20). However, the mechanism by which Dorfin discriminates between the normal and pathogenic status of SOD1 proteins remains unknown. There are numerous variants causing familial ALS, thus it seems reasonable that Dorfin recognizes a common protein modification among mutant SOD1s that is not present in wild-type SOD1.

* This work was supported by a Center of Excellence grant from the Ministry of Education, Culture, Sports, Science and Technology and grants from the Ministry of Health, Labor and Welfare of Japan. The costs of publication of this article were defrayed in part by the payment of page charges. This article must therefore be hereby marked "*advertisement*" in accordance with 18 U.S.C. Section 1734 solely to indicate this fact.

[S] The on-line version of this article (available at http://www.jbc.org) contains supplemental Fig. S1.

[1] To whom correspondence should be addressed. Tel.: 81-52-744-2385; Fax: 81-52-744-2384; E-mail: sobueg@med.nagoya-u.ac.jp.

[2] The abbreviations used are: SOD1, superoxide dismutase 1; ALS, amyotrophic lateral sclerosis; 2-ME, 2-mercaptoethanol; WST-1, 4-[3-(4-iodophenyl)-2-(4-nitrophenyl)-2H-5-tetrazolio]-1,3-benzene disulfonate; GFP, green fluorescent protein.

In this study, we generated SOD1 proteins with various combinations of the four Cys residues replaced by serines and assessed their disulfide bond status, the changes in the formations of their high molecular weight species, and their neurotoxicity. Moreover, by studying the interaction between Dorfin and these engineered SOD1s, we investigated whether disulfide bonds are critical for Dorfin recognition and ubiquitylation of mutant SOD1s.

EXPERIMENTAL PROCEDURES

Construction of Expression Vectors—Construction of pcDNA3.1/MycHis-SOD1, pEGFP-N1-SOD1, and pcDNA4/HisMax-Dorfin vectors were described previously (20, 22). Cys to Ser missense mutations were introduced into pcDNA3.1/MycHis-SOD1 and pEGFP-N1-SOD1 with a QuikChange site-directed mutagenesis kit (Stratagene, La Jolla, CA). Primer pairs for each Cys to Ser mutant were as follows: 5′-CGAAGGCCGTGTCCGTGCTGAAGGGC-3′ and 5′-GCCCTTCAGCACGGACACGGCCTTCG-3′ for C6S; 5′-GATAATACAGCAGGCTCTACCAGTGCAGGTCC-3′ and 5′-GGACCTGCACTGGTAGAGCCTGCTGTATTATC-3′ for C57S; 5′-CTCAGGAGACCATTCCATCATTGGCCGCAC-3′ and 5′-GTGCGGCCAATGATGGAATGGTCTCCTGAG-3′ for C111S; and 5′-GGAAGTCGTTTGGCTTCTGGTGTAATTGGGATCG-3′ and 5′-CGATCCCAATTACACCAGAAGCCAAACGACTTCC-3 for C146S. Multiple Cys to Ser replaced vectors were obtained by repeatedly applying a mutagenesis.

Cell Culture, Transfection, and Antibodies—Neuro-2a cells (American Type Culture Collection, Manassas, VA), a line derived from mouse neuroblastoma, were maintained in Dulbecco's modified Eagle's medium containing 10% fetal calf serum, 5 units/ml penicillin, and 50 μg/ml streptomycin. Transfections were performed using Lipofectamine 2000 (Invitrogen) in the WST-1 assay or Effectene Transfection Reagent (Qiagen, Valencia, CA) in other experiments according to the manufacturers' instructions. To inhibit cellular proteasome activity, cells were treated with 1 μM (except as otherwise indicated) MG132 (Z-Leu-Leu-Leu-al, Sigma) or epoxomicin (Sigma) as indicated concentration for 24 h after overnight transfection. To differentiate Neuro-2a cells, they were changed to Dulbecco's modified Eagle's medium culture medium containing 2% fetal calf serum and 20 μM retinoic acid and cultured for 48 h. Primary antibodies used were as follows: anti-Myc mouse monoclonal antibody (9E10, Sigma), anti-Myc rabbit polyclonal antibody (A-14, Santa Cruz Biotechnology, Santa Cruz, CA), anti-SOD1 rabbit polyclonal antibody (SOD100, Stressgen Bioreagents, Victoria, Canada), anti-α-tubulin mouse monoclonal antibody (B-5-1-1, Sigma), anti-ubiquitin mouse monoclonal antibody (4PD1, Santa Cruz Biotechnology), and anti-Xpress mouse monoclonal antibody (Invitrogen).

Transgenic Mice—17-week-old symptomatic B6SJL-TgN(SOD1-G93A)1Gur ALS mice overexpressing the human mutant $SOD1^{G93A}$ (The Jackson Laboratory, Bar Harbor, ME) were used. The experimental design of this study was fully approved by the Experimental Animal Ethical Committee of the Nagoya University Graduate School of Medicine. Tissues were homogenized in 10 volumes of lysis buffer (TNE) consisting of 50 mM Tris-HCl, 150 mM NaCl, 1% Nonidet P-40, and 1 mM EDTA with a protease inhibitor mixture (Complete Mini, Roche Diagnostics, Indianapolis, IN) and centrifuged at 20,000 × *g* for 30 min at 4 °C. Supernatants were used for Western blotting analysis.

Immunoprecipitation and Western Blotting Analysis—5×10^5 cells from a 6-cm dish were lysed on ice with 1 ml of TNE lysis buffer. The lysate was centrifuged at 1,000 × *g* for 15 min at 4 °C to remove nuclei and cell debris. Denucleated cell lysates (crude fraction) were separated into supernatant (soluble fraction) and pellet fractions by centrifuging at 20,000 × *g* for 20 min at 4 °C. The pellets were lysed (insoluble fraction) with 1 ml of TNES lysis buffer consisting of 50 mM Tris-HCl, 150 mM NaCl, 1% Nonidet P-40, 2% SDS, and 1 mM EDTA with a protease inhibitor mixture (Complete Mini, Roche Diagnostics). Protein concentrations were determined with a DC protein assay kit (Bio-Rad). Immunoprecipitation from the soluble fraction was performed with 2 μg of anti-Myc or anti-Xpress antibodies and Protein A/G Plus-agarose (Santa Cruz Biotechnology), and the precipitates were washed four times in TNE buffer. Cell lysates or immunoprecipitates were separated by SDS-PAGE (5–20% gradient gel) and analyzed by Western blotting with ECL plus detection reagents (GE Healthcare Bio-Sciences, Piscataway, NJ). Non-reducing SDS-PAGE was conducted without 2-mercaptoethanol (2-ME) in the sample buffer. Because omitting reducing agents from the protein samples can lead to adventitious air oxidation or disulfide scrambling, 100 mM iodoacetamide was added to the lysates to prevent these changes during sample preparation.

Filter Trap Assay—Each of the various fractions from the cell lysates (crude, soluble, and insoluble fractions) was filtered under vacuum through 0.2-μm cellulose acetate membranes (Sartorius, Gottingen, Germany) followed by two washes in Tris-buffered saline. The membranes were then incubated with 5% milk powder in Tris-buffered saline at room temperature for 1 h, followed by an overnight incubation at 4 °C with anti-Myc antibody in Tris-buffered saline with 0.1% Tween 20. Primary antibodies were detected with horseradish peroxidase-conjugated secondary antibodies (GE Healthcare Bio-Sciences), which were then detected with ECL plus chemiluminescence reagent (GE Healthcare Bio-Sciences). To confirm equal loading of proteins, the same samples were blotted onto 0.45-μm nitrocellulose membranes (Bio-Rad) and probed with anti-Myc or anti-α-tubulin antibodies.

Neurotoxicity Analysis and Quantification of SOD1 Aggregates—2×10^4 Neuro-2a cells were grown overnight on four-chamber, collagen-coated slides (Nalge Nunc, Rochester, NY) and then transfected with 0.2 μg of pEGFP-N1-SOD1. After overnight incubation, the cells were differentiated in Dulbecco's modified Eagle's medium containing 2% fetal calf serum and 20 μM retinoic acid for 48 h. Inclusion bodies were counted in more than 100 randomly selected cells, and the percentages of cells with such inclusions were calculated. Data from three independent experiments were averaged. For the cell viability assay, 5×10^3 Neuro-2a cells were grown in 96-well collagen-coated plates overnight, and then transfected with 0.1 μg of pEGFP-N1-SOD1 or pcDNA3.1/MycHis-SOD1, with or without 0.1 μg of pcDNA4/HisMax-Dorfin. pcDNA4/HisMax

mock vector was used as a control. A 4-[3-(4-iodophenyl)-2-(4-nitrophenyl)-2H-5-tetrazolio]-1,3-benzene disulfonate (WST-1)-based cell proliferation assay (Roche Diagnostics) was performed 48 h after differentiation. Absorbance was measured in a multiple plate reader (PowerscanHT, Dainippon Pharmaceutical, Japan). The assay was carried out in triplicate and statistically analyzed by one-way analysis of variance or unpaired *t* test.

Quantitative Analysis of Gene Expression Levels—Total RNA was extracted from Neuro-2a cells expressing SOD1-GFP and their Cys to Ser derivatives by using an RNA Easy Kit (Qiagen), followed by cDNA synthesis primed with oligo(dT) using Superscript II (Invitrogen). The gene expression level was examined by quantitative reverse transcription-PCR using primer sets specific to target genes and QuantiTect SYBR Green PCR kit (Qiagen). PCR was performed on an iCycler system (Bio-Rad) under the manufacturer's recommended conditions.

Isolation of SOD1 Aggregates—Isolation of SOD1 inclusion bodies was carried out according to Lee *et al.* (24) with a slight modification. 5×10^5 Neuro-2a cells in a 60-mm dish expressing SOD1-GFP were washed with cold phosphate-buffered saline before addition of TNE buffer. After a 5-min incubation at room temperature, the supernatant containing Nonidet P-40-soluble proteins was carefully removed from dishes. After gentle washing of dishes with phosphate-buffered saline, the Nonidet P-40-insoluble materials were scraped and incubated on ice for 5 min. The extract was then centrifuged at $80 \times g$ for 15 min. The pellet containing big inclusions was put onto a slide glass, sealed with a coverslip, and observed under a BX51 epifluorescence microscope (Olympus, Tokyo, Japan).

Cycloheximide Chase Analysis—Neuro-2a cells grown on 6-cm dishes were transfected with 1 μg of pcDNA3.1/MycHis-SOD1 with or without 1 μg of pcDNA4/HisMax-Dorfin. 24 h after transfection, cycloheximide (50 μg/ml) was added to the culture medium, and the cells were harvested at the indicated time points. The samples were subjected to SDS-PAGE and analyzed by Western blotting with anti-Myc antibody. The intensities of the bands were quantified by Image-Gauge software (Fuji Film, Tokyo, Japan). The assay was carried out in triplicate and statistically analyzed by one-way analysis of variance or unpaired *t* test.

RESULTS

Proteasome Inhibition Increases SDS-resistant Disulfide-linked Species as Well as Insoluble Ones of ALS-linked Mutant SOD1—Mutant SOD1 is a fairly unstable protein, and the increased turnover of mutant SOD1 is mediated by the ubiquitin-proteasome pathway (18, 19). Thus, we first examined the effect of proteasome inhibition on mutant SOD1 proteins. When cellular proteasome activity was blocked by the proteasome inhibitor MG132, the level of soluble mutant $SOD1^{G85R}$ and $SOD1^{G93A}$ increased in a dose-dependent manner (Fig. 1*B*, *arrowhead*), and an SDS-resistant mutant SOD1 dimer appeared (Fig. 1*B*, *arrow*). The increase in the amount of wild-type SOD1 was much smaller than that of mutant SOD1 (Fig. 1*B*, *arrowhead*). Detergent-insoluble, sedimentable mutant SOD1 also increased as proteasome activity was inhibited (Fig. 1*C*). Interestingly, as the proteasome activity was inhibited, aberrant high molecular weight SDS-resistant disulfide-linked mutant $SOD1^{G85R}$ and $SOD1^{G93A}$ became more abundant (Fig. 1*A*, *asterisk*). There were almost no SDS-resistant disulfide-linked species of the wild-type SOD1. The same findings were obtained when blots were probed with anti-SOD1 antibody (supplemental Fig. S1*A*). These results were also confirmed with epoxomicin, a selective and irreversible proteasome inhibitor (supplemental Fig. S1*B*). Thus, intermolecular disulfide bond-linked mutant SOD1 is unstable and prone to degradation by the proteasome.

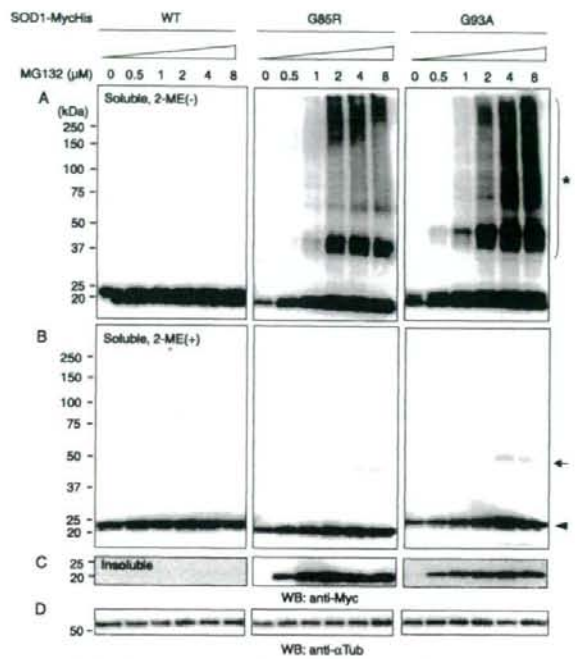

FIGURE 1. **Proteasome inhibition leads to the accumulation of intermolecular disulfide bond-linked mutant SOD1.** Neuro-2a cells expressing wild-type (*WT*), G85R, and G93A mutant SOD1-MycHis were treated with MG132 for 24 h at the indicated concentrations. Soluble fractions were analyzed by SDS-PAGE in the absence (*A*) or presence (*B*) of 2-ME. Insoluble fractions were analyzed by SDS-PAGE in the presence of 2-ME (*C*). *Arrow*, a soluble SDS-resistant dimer; *arrowhead*, a soluble monomeric SOD1; *asterisk*, disulfide-linked high molecular weight-species of SOD1. *D*, anti-α-tubulin as loading control.

Free Cys^6 and Cys^{111} Are Important for Generating Disulfide Bond-linked Species and Insoluble, Sedimentable Forms of Mutant Human SOD1—We examined the role of Cys residues in the formation of aberrant disulfide-bond linked high molecular weight species. Various combinations of the four Cys residues at positions 6, 57, 111, and 146 replaced with serines were introduced into SOD1 protein-expression vectors using site-directed mutagenesis. The effects of amino acid replacement at one of the four Cys residues, at two of the four Cys residues, and at all four Cys residues on wild-type and two familial ALS-linked SOD1 mutants, $SOD1^{G85R}$ and $SOD1^{G93A}$, were investigated. We used Myc-His-tagged SOD1 expression vectors and an antibody against the tag peptide to detect SOD1 protein so as to avoid possible reduced detection of SOD1 with multiple